MycoKeys 101: 45–80 (2024)
DOI: 10.3897/mycokeys.101.113128

Research Article

Morphological and phylogenetic analyses reveal three new species of *Fusarium* (Hypocreales, Nectriaceae) associated with leaf blight on *Cunninghamia lanceolata* in China

Jiao He[1], De-Wei Li[2], Wen-Li Cui[1], Li-Hua Zhu[1], Lin Huang[1]

1 *Co-Innovation Center for Sustainable Forestry in Southern China, Nanjing Forestry University, Nanjing, Jiangsu 210037, China*
2 *The Connecticut Agricultural Experiment Station Valley Laboratory, Windsor, CT 06095, USA*
Corresponding author: Lin Huang (lhuang@njfu.edu.cn)

Abstract

Chinese fir (*Cunninghamia lanceolata*) is a special fast-growing commercial tree species in China with high economic value. In recent years, leaf blight disease on *C. lanceolata* has been observed frequently. The diversity of *Fusarium* species associated with leaf blight on *C. lanceolata* in China (Fujian, Guangxi, Guizhou, and Hunan provinces) was evaluated using morphological study and molecular multi-locus analyses based on RNA polymerase second largest subunit (*RPB2*), translation elongation factor 1-alpha (*TEF-1α*), and RNA polymerase largest subunit (*RPB1*) genes/region as well as the pairwise homoplasy index tests. A total of five *Fusarium* species belonging to four *Fusarium* species complexes were recognized in this study. Two known species including *Fusarium concentricum* and *F. fujikuroi* belonged to the *F. fujikuroi* species complex, and three new *Fusarium* species were described, i.e., *F. fujianense* belonged to the *F. lateritium* species complex, *F. guizhouense* belonged to the *F. sambucinum* species complex, and *F. hunanense* belonged to the *F. solani* species complex. To prove Koch's postulates, pathogenicity tests on *C. lanceolata* revealed a wide variation in pathogenicity and aggressiveness among the species, of which *F. hunanense* HN33-8-2 caused the most severe symptoms and *F. fujianense* LC14 led to the least severe symptoms. To our knowledge, this study also represented the first report of *F. concentricum*, *F. fujianense*, *F. fujikuroi*, *F. guizhouense*, and *F. hunanense* causing leaf blight on *C. lanceolata* in China.

Key words: *Cunninghamia lanceolata*, *Fusarium*, leaf blight, new species, pathogenicity

Academic editor: Ning Jiang
Received: 23 September 2023
Accepted: 12 December 2023
Published: 8 January 2024

Citation: He J, Li D-W, Cui W-L, Zhu L-H, Huang L (2024) Morphological and phylogenetic analyses reveal three new species of *Fusarium* (Hypocreales, Nectriaceae) associated with leaf blight on *Cunninghamia lanceolata* in China. MycoKeys 101: 45–80. https://doi.org/10.3897/mycokeys.101.113128

Introduction

The genus *Fusarium* (Nectriaceae) is one of the most renowned genera that contains many phytopathogenic fungi. The members of this genus can directly incite diseases in plants, humans, and domesticated animals (Rabodonirina et al. 1994; Boonpasart et al. 2002; Vismer et al. 2002). *Fusarium* was included in the top 10 globally most important genera of plant pathogenic fungi based on scientific and economic importance (Dean et al. 2012), in particular because of the members of the *F. sambucinum* species complex (FSAMSC) and *F. oxysporum* species complex (FOSC) (O'Donnell et al. 2015; Gräfenhan et al. 2016)

that comprises some of the most destructive agricultural pathogens. *Fusarium graminearum* and 21 related species comprising the *F. sambucinum* species complex lineage 1 (FSAMSC-1) are the most important *Fusarium* head blight (FHB) pathogens of cereal crops world-wide (Goswami and Kistler 2005; Kelly et al. 2016). Further impactful fusaria include the members of the *F. fujikuroi* species complex (FFSC), *F. verticillioides* (teleomorphic synonym, *Gibberella moniliformis*), *F. fujikuroi* (teleomorphic synonym, *G. fujikuroi*), and *F. proliferatum* (teleomorphic synonym, *G. intermedia*), which are well known for their abilities to cause devastating diseases, such as rice bakanae, maize ear rot and soybean root rot, leading to considerable reductions in crop yields and economic income (O'Donnell et al. 2015; Qiu et al. 2020). The members of the *F. solani* species complex (FSSC) cause plant diseases, mostly root and crown rots and vascular wilts on a wide range of plants, including soybeans, potato, cucurbits, peas, sweet potato, Chinese rose, and various legumes (Coleman 2016; Summerell 2019; He et al. 2021).

There has been confusion in *Fusarium* taxonomy for a long time because of the nine-species system of Snyder and Hansen (1940), the misleading overlaps caused by convergent evolution and character loss, the phenomenon of cultural degeneration, and firm opinions of the taxonomists and plant pathologists who have been working on them. First described by Link (1809) and typified by *Fusarium roseum* (presently *F. sambucinum* nom. cons.) (Gams et al. 1997), the generic and species concepts in *Fusarium* have endured significant changes since the cornerstone of phenotypically-based taxonomic treatments that grouped species into sections, morphological varieties or forms and later formae speciales based on pathogenicity and host ranges (Wollenweber and Reinking 1935; Snyder and Hansen 1940; Toussoun and Nelson 1968; Gerlach and Nirenberg 1982; Nelson et al. 1983; Burgess et al. 1988). Later, the species were redistributed into species complexes after the introduction of modern molecular tools (O'Donnell et al. 2000; Geiser et al. 2013; O'Donnell et al. 2013; Aoki et al. 2014). O'Donnell et al. (2022) indicates that *Fusarium* is assessed to have >400 phylospecies and *ca*. 1/3 of the phylospecies have not been formally described; clearly, morphology alone is insufficient to differentiate most of these species. To solve the species delimitation and identification dilemma, a polyphasic approach has gradually been applied and several online databases (*Fusarium*-ID, *Fusarium* MLST and FUSARIOID-ID) have been established based on different taxonomic opinions (O'Donnell et al. 2012; Crous et al. 2021; Torres-Cruz et al. 2022). Despite these significant contributions, debates surrounding the generic delimitation of *Fusarium* and whether the genus *Neocosmospora* (also known as *F. solani* species complex, FSSC) belongs to *Fusarium* remain (Crous et al. 2021; Geiser et al. 2021; Wang et al. 2022). There has been a consensus for over a century that the FSSC is part of *Fusarium*, which was affirmed by molecular phylogenetic analyses and codified in a proposal to recognize *Fusarium* as a monophyletic group that includes the FSSC (Geiser et al. 2013). A disagreement on the generic concept of *Fusarium* has become more contentious in the last decade. Geiser et al. (2013) advocated "recognizing the genus *Fusarium* as the sole name for a group that includes virtually all *Fusarium* species of importance in plant pathology, mycotoxicology, medicine, and basic research", and the retained genus *Fusarium* includes *F. solani* species complex (FSSC). This treatment was subsequently challenged by Lombard

et al. (2015) who split the genus *Fusarium* into seven genera and segregated the FSSC as *Neocospmospora*. Later, Sandoval-Denis and Crous (2018) and Sandoval-Denis et al. (2019) justified the treatment of Lombard et al. (2015) based on the phylogenetic analyses using four loci and dispute that the Geiser et al. (2013) concept of *Fusarium* is polyphyletic. O'Donnell et al. (2020) rebutted the polyphyletic conclusions of Sandoval-Denis and Crous (2018) and Sandoval-Denis et al. (2019). Geiser et al. (2021) examined the conclusion of Sandoval-Denis and Crous (2018) and Sandoval-Denis et al. (2019), developed a phylogeny according to sequences of 19 orthologous protein-coding genes and show that *Fusarium* including the FSSC is monophyletic. Thus, 40 species described as *Neocosmospora* are recently recombined in *Fusarium* (Aoki et al. 2020, 2021a, b). Crous et al. (2021) insist that fusarium-like are polyphyletic in Nectriaceae and dispute that a narrower generic concept with a combination of features is necessary for the majority of fusarioid species based on the phylogenetic analyses using sequence data of eight loci. They segregate the Wollenweber concept of *Fusarium* into 20 genera with synapomorphic characteristics (Crous et al. 2021). O'Donnell et al. (2022) opined that *Fusarium* remains the best scientific, nomenclatural and practical taxonomic option available. However, the disagreement is far from settled.

The narrow generic concept of *Fusarium* is leading to a large number of name changes and confusions among plant pathologists, medical mycologists, quarantine officials, regulatory agencies, biologists, and other professionals. Rebuilding the correct systematic position of a large number of fungal names cannot be achieved without repeated studies (de Hoog et al. 2023). The purpose of choosing *Fusarium*, not *Neocosmospora* or other generic names is to maintain the stability of the name *Fusarium* in plant pathology and minimize confusion. We hope more independent studies in the future will resolve the phylogenetic disputes on *Fusarium s. l.*

Morphology is a fundamental component of the generic and species concepts of fungi and must not be overlooked. Key morphological features for generic circumscription include characteristics of sexual morphs such as perithecial morphology, the presence and nature of a basal stroma, ascus characters, and ascospore shape, septation, color as well as surface ornamentation (Rossman et al. 1999), but sexual stage rarely develop. Therefore, diagnostic characters are the dimensions and characteristics of aerial conidiophores and conidiogenous cells (mono- vs. poly-phialides), presence/absence and characteristics of sporodochia, the types of conidia produced, e.g., aerial microconidia, and aerial and sporodochial macroconidia. Finally, the presence or absence of chlamydospores may be important (Leslie and Summerell 2006). However, the morphology of fungal structures will vary dramatically depending on the selection of media and growth conditions, which may compromise the identification process, and some *Fusarium* strains are similar in colony morphology and biology, which also makes it difficult to directly differentiate strains (Crous et al. 2021).

Current *Fusarium* taxonomy is dominated by molecular phylogenetic studies. Many protein-coding genes have been explored for identification and taxonomic purposes in *Fusarium*. The 28S large subunit (LSU) nrDNA, internal transcribed spacer region and intervening 5.8S nrRNA gene (ITS), large subunit of the ATP citrate lyase (*acl1*), RNA polymerase II largest subunit (*rpb1*), RNA polymerase II second largest subunit (*rpb2*), α-actin (*act*), β-tubulin (*tub2*), calmodulin

(*cmdA*), histone H3 (*his3*), and translation elongation factor 1-alpha (*tef1*) loci are currently used (Lombard et al. 2015; Sandoval-Denis et al. 2018; Crous et al. 2021). However, *TEF-1α* and *RPB2* sequences appear to be the most useful in taxonomic studies of fungi of the *Fusarium* genus. Both offer high discriminatory power and are well represented in public databases (O'Donnell 2000). *TEF-1α* is commonly the first-choice identification marker as it has very good resolution power for most species, while *RPB2* allows for enhanced discrimination between closely related species (Crous et al. 2021). Additional genetic markers, often employed in association with the previously mentioned genes in multigene phylogenetic analyses, include *TUB2*, *HIS3*, *CAM*, and *RPB1*. These markers have variable resolution or applicability depending on the genus or species complex (Crous et al. 2021). One of the latest studies has used 19 loci to provide a much better phylogeny of *Fusarium* (Geiser et al. 2021). At present, Genealogical Concordance Phylogenetic Species Recognition (GCPSR) (Taylor et al. 2000) based multilocus data analyses have resolved *Fusarium* into >400 phylogenetically distinct species distributed among 23 monophyletic species complexes and several single-species lineages (O'Donnell et al. 2015; Summerell 2019; O'Donnell et al. 2020; Geiser et al. 2021).

Chinese fir (*Cunninghamia lanceolata* (Lamb.) Hook.) is an evergreen coniferous tree species. Because of its fast growth, straight trunk, and high economic value, it is widely cultivated in the Yangtze River Basin and the southern Qinling Mountains in China. It is the main afforestation tree species in southern China. Average timber volume is estimated at 500–800 m^3/ha, and in China, *C. lanceolata* contributes 40% of the total commercial timber production (Zheng et al. 2016). However, *C. lanceolata* is often damaged by many diseases and insect pests (Lan et al. 2015). Some common insect pests include *Semanotus sinoauster*, *Callidium villosulum*, and *Lobesia cunninghamiacola* (Lan et al. 2015). *Bartalinia cunninghamiicola*, *Berkeleyomyces basicola* (≡ *Thielaviopsis basicola*), *Bipolaris oryzae*, *Bi. setariae*, *Ceratocystis acaciivora*, *Chalaropsis* sp., *Colletotrichum cangyuanense*, *C. fructicola*, *C. gloeosporioides*, *C. kahawae*, *C. karstii*, *C. siamense*, *Curvularia spicifera*, *Cur. muehlenbeckiae*, *Ceratocystis collisensis*, *Diaporthe anhuiensis*, *Dia. citrichinensis*, *Dia. unshiuensis*, *Dia. hongkongensis*, *Discosia pini*, *Lophodermium uncinatum*, *Nigrospora sphaerica*, *Rhizoctonia solani*, *Fusarium oxysporum* f. *pini*, and *Fusarium* sp. have been reported as pathogens on *C. lanceolata* (Anonymous 1979; Kobayashi and Zhao 1987; Wang et al. 1995; Chen 2002; Lan et al. 2015; Liu et al. 2015; Xu and Liu 2017; Huang et al. 2018; Tian et al. 2019; Zhou and Hou 2019; Cui et al. 2020a, b; He et al. 2022; Li et al. 2022; Dai et al. 2023; Liao et al. 2023).

An investigation of fungal diseases on leaves of *C. lanceolata* covering its main cultivation regions of *C. lanceolata* in China was conducted from 2016 to 2020 (unpublished data) and samples of leaf blight were collected. The foliar symptoms ranged from leaf spots, anthracnose to leaf blight. The leaf blight disease mainly caused pale brown to brownish necrotic needles on *C. lanceolata*. Our preliminary study showed that a number of fungi were responsible for the foliar diseases of *C. lanceolata* in the field, including *Alternaria* spp., *Bipolaris* spp., *Colletotrichum* spp., *Curvularia* spp., *Fusarium* spp., and *Pestalotiopsis* spp. The main aim of the present study is to determine the *Fusarium* spp. associated with *C. lanceolata*.

Materials and methods

Isolation of the potential fungal pathogen

A total of 20 isolates of *Fusarium* spp. were isolated from leaf blight disease samples of *C. lanceolata*, which were collected in four provinces (Fujian, Guangxi, Guizhou, and Hunan) in China (Suppl. material 1: table S1). Small sections (2 × 3 mm) were cut from the margins of infected tissues and surface sterilized in 75% alcohol for 30 s, then in 1% sodium hypochlorite (NaOCl) for 90 s, followed by three rinses with sterile water (Huang et al. 2016), then blotted dry with sterilized filter paper, placed on 2% potato dextrose agar (PDA) Petri plates with 100 mg/L ampicillin, and then cultured for 3 days at 25 °C in the dark. Fungal isolates were purified with the monosporic isolation method described by Li et al. (2007) using the spores produced with liquid cultures. Single-spore isolates were maintained on PDA plates. The obtained isolates were stored in the Forest Pathology Laboratory at Nanjing Forestry University. Holotype specimens of new species from this study were deposited at the China Forestry Culture Collection Center (**CFCC**), Chinese Academy of Forestry, Beijing, China.

DNA extraction, PCR amplification and sequencing

Genomic DNA of 20 isolates was extracted using a modified CTAB method (Damm et al. 2008). The fungal plugs of each isolate were grown on the PDA plates for 5 days and then collected in a 2 mL tube. Then, 500 µL of chloroform and 500 µL of hexadecyltrimethyl ammonium bromide (CTAB) extraction buffer (0.2 M Tris, 1.4 M NaCl, 20 mM EDTA, 0.2 g/L CTAB) were added into the tubes, which were placed in a shaker at 25 °C at 200 rpm for 2-h. The mixture was centrifuged at 15,800 × *g* for 5 min. Then, 300 µL of the supernatant was transferred into a new tube, and 600 µL of 100% ethanol was added. The suspension was centrifuged at 15,800 × *g* for 5 min. At that point, 600 µL of 70% ethanol was added into the precipitate. The suspension was centrifuged at 15,800 × *g* for 5 min, and the supernatant was discarded. The DNA pellet was dried and re-suspended in 30 µL ddH_2O.

The polymerase chain reaction (PCR) amplification was carried out on the extracted DNA. *TEF-1α*, *RPB2*, and *RPB1* were amplified with the primer sets of EF1/EF2 (O'Donnell et al. 1998), 5f2/7cr (Liu et al. 1999), and Fa/G2R (O'Donnell et al. 2010), respectively. The primer sequences were listed in Suppl. material 1: table S2.

PCR was performed in a 30 µl reaction volume containing 2 µL of genomic DNA (*ca*. 200 ng/µL), 15 µL of 2× Taq Plus Master Mix (Dye Plus) (Vazyme P212-01), 1 µL of 10 µM forward primer, 1 µL of 10 µM reverse primer, and 11 µL of ddH_2O. The parameters for PCR protocol were 94 °C for 4 min, followed by 34 cycles of 30 s at 94 °C, annealing at a suitable temperature for the 30 s for different loci: 55 °C for *TEF-1α*, *RPB2*, and *RPB1*, 72 °C for 60 s, and a final elongation step at 72 °C for 10 min. All DNA sequencing was performed at Shanghai Sangon Biotechnology Company (Nanjing, China). The sequences derived in this study were deposited in GenBank. GenBank accession numbers of all isolates used for phylogenetic analyses were listed in Table 1.

Table 1. Cultures, specimens and DNA accession numbers included in this study.

Species name	Culture/specimen[1]	Host	Country/area	GenBank/ENA accession number[2]		
				TEF–1α	RPB2	RPB1
***Fusarium fujikuroi* species complex**						
F. acutatum	CBS 402.97^{T} (Ex-type)	Unknown	India	KR071754	KT154005	MT010947
F. agapanthi	NRRL 54463^{HT} (Ex-holotype)	African lily	Australia and Italy	KU900630	KU900625	KU900620
	NRRL 54464^{HT}	African lily	Australia and Italy	–	KU900627	KU900622
F. ananatum	CBS 118516^{T}	Unknown	Unknown	–	KU604269	MT010937
F. awaxy	LGMF 1930^{HT}	stalk, *Zea mays*	Brazil	MG839004	MK766941	–
F. bactridioides	CBS 100057^{T}	*Pinus leiophylla*	Arizona, USA	KC514053	–	MT010939
F. begoniae	CBS 452.97^{T}	Begonia elatior hybrid	Germany	KC514054	MT010964	–
F. brevicatenulatum	CBS 404.97^{T}	*Striga asiatica*	Madagascar	MT011005	MT010979	MT010948
	NRRL 25447^{T}	Unknown	Unknown	MN193859	MN193887	–
F. concentricum	MUCL 55980	*Musa* sp.	China	LT574935	LT575016	–
	MUCL 55983	*Musa* sp.	China	LT574938	LT575019	–
	CBS 450.97^{T}	*Musa sapientum* fruit	Costa Rica	MT010992	MT010981	MT010942
	SJ1-10 *	Chinese fir	China	ON734385	ON734365	OR683264
	SJ1-10-1 *	Chinese fir	China	ON734386	ON734366	OR683265
	SJ1-10-2 *	Chinese fir	China	ON734387	ON734367	OR683266
	SJ1-10-3 *	Chinese fir	China	ON734388	ON734368	OR683267
F. circinatum	NRRL 25331^{T} = CBS 405.97	Monterrey pine tree	USA	AF160295	JX171623	–
F. fujikuroi	HJYB-4	*Zanthoxylum armatum*	China	MT902140	MT902141	–
	MUCL 55986	*Musa* sp.	China	LT574941	LT575022	–
	CBS 221.76^{T}	*Oryza sativa* culm	Taiwan	KR071741	KU604255	–
	HN43-17-1 *	Chinese fir	China	ON734397	ON734377	OR683276
	HN43-17-1-1 *	Chinese fir	China	ON734398	ON734378	OR683277
	HN43-17-1-2 *	Chinese fir	China	ON734399	ON734379	OR683278
	HN43-17-1-3 *	Chinese fir	China	ON734400	ON734380	OR683279
F. lactis	NRRL 25200^{NT} = CBS 411.97 (Ex-neotype)	*Ficus carica*	USA	AF160272	–	MT010954
F. mangiferae	NRRL 25226^{T} = BBA 69662	*Mangifera indica*	India	AF160281	JX171622	–
F. nygamai	NRRL 13448^{T} = CBS 749.97	Necrotic sorghum root	Australia	AF160273	EF470114	MT010955
F. pseudocircinatum	NRRL 22946^{T} = CBS 126.73	*Solanum* sp.	Ghana	AF160271	–	MT010952
F. pseudonygamai	NRRL 13592^{T} = CBS 417.97	*Pennisetum typhoides*	Nigeria	AF160263	–	MT010951
F. ramigenum	NRRL 25208^{T} = CBS 418.97	*Ficus carica*	USA	AF160267	KF466412	MT010959
F. sacchari	NRRL 13999 = CBS 223.76	*Saccharum officinarum*	India	AF160278	JX171580	–
F. subglutinans	NRRL 22016^{T} = CBS 747.97	Corn	USA	AF160289	JX171599	–
F. thapsinum	NRRL 22045 = CBS 733.97	*Sorghum bicolor*	South Africa	AF160270	JX171600	–
F. udum	NRRL 22949 = CBS 178.32	unknown	Germany	AF160275	–	–
F. xyrophilum	NRRL 62721	*Xyris* spp.	Guyana	–	MN193905	MW402721
	NRRL 62710	*Xyris* spp.	Guyana	–	MN193903	MW402720
F. zealandicum (Outgroup)	CBS 111.93^{T}	*Hoheria populnea* bark	New Zealand	HQ728148	HM626684	–
***F. lateritium* species complex**						
F. cassiae	MFLUCC 18-0573^{HT}	*Cassia fistula*	Thailand	MT212205	MT212197	–
F. citri-sinensis	YZU 191316^{T}	*Citrus sinensis* fruit	China	MW855826	MW855854	–
	YZU 181391	*Citrus sinensis* fruit	China	MW855825	OM913582	–
F. fujianense	LC14 *	Chinese fir	China	ON734389	ON734369	OR683268
	LC14-1 *	Chinese fir	China	ON734390	ON734370	OR683269
F. fujianense	LC14-2 *	Chinese fir	China	ON734391	ON734371	OR683270
	LC14-3 *	Chinese fir	China	ON734392	ON734372	OR683271
F. lateritium	NRRL 52786	unknown	Germany	JF740854	JF741180	JF741009
F. lateritium	NRRL 25122^{LT} (Ex-lectotype)	unknown	Germany	JF740747	JF741075	JF740959

Species name	Culture/specimen[1]	Host	Country/area	GenBank/ENA accession number[2]		
				TEF–1α	RPB2	RPB1
F. magnoliae-champaca	MFLUCC 18-0580^{HT}	*Magnolia champaca*	Thailand	–	MT212198	–
F. massalimae	URM 8239^{T}	*Handroanthus chrysotrichus*	Brazil	MN939763	MN939767	–
	FCCUFG 05^{HT}	*Handroanthus chrysotrichus*	Brazil	MN939764	MN939768	–
F. sarcochroum	CPC 28118	*Citrus limon*	Castellò, Spain	LT746213	LT746326	LT746298
	CPC 28075^{NT}	*Citrus reticulata*	Alginet, Spain	LT746211	LT746324	LT746296
F. stilboides	CBS 746.79^{T}	*Citrus* sp.	New Zealand	MW928843	MW928832	–
F. sublunatum (Outgroup)	CBS 189.34^{T}	*Musa sapientum* and *Theobroma cacao*	USA	–	KM232380	–
***F. sambucinum* species complex**						
F. acaciae-mearnsii	NRRL 26754^{T}	*Acacia mearnsii*	South Africa	AF212448	KM361658	KM361640
F. aethiopicum	NRRL 46718	wheat seed	Ethiopia	FJ240296	KM361670	KM361652
	NRRL 46726	wheat seed	Ethiopia	MW233126	MW233470	MW233298
	NRRL 6227	*Triticum aestivum*	New South Wales, Australia	HM744692	JX171560	JX171446
	FRC R09335	*Triticum aestivum*	New South Wales, Australia	GQ915501	GQ915485	–
F. concentricum (Outgroup)	CBS 450.97^{T}	*Musa sapientum* fruit	Costa Rica	–	MT010981	MT010942
F. cortaderiae	NRRL 29297	*Cortaderia* sp.	New Zealand	MW233098	MW233442	MW233270
F. culmorum	NRRL 25475^{T}	Barley	Denmark	MW233082	MW233425	MW233253
F. guizhouense	GZ7-20-1 *	Chinese fir	China	ON734381	ON734361	OR683260
	GZ7-20-1-1 *	Chinese fir	China	ON734382	ON734362	OR683261
	GZ7-20-1-2 *	Chinese fir	China	ON734383	ON734363	OR683262
	GZ7-20-1-3 *	Chinese fir	China	ON734384	ON734364	OR683263
F. graminearum	NRRL 31084	unknown	unknown	MW233103	JX171644	JX171531
F. langsethiae	NRRL 53439	oat kernel	Norway	HM744691	HQ154479	–
F. longipes	NRRL 20695	soil	USA	GQ915509	GQ915493	–
F. louisianense	NRRL 54197	*Triticum aestivum*	USA	KM889633	MW233478	MW233306
F. mesoamericanum	NRRL 25797	*Musa* sp.	Honduras	AF212441	MW233426	MW233254
F. poae	LC6917	*Oryza sativa*	China	MW620088	MW474613	MW024655
	LC13783	*Hordeum vulgare*	China	MW620087	MW474612	MW024654
	NRRL 26941^{T}	Barley	USA	–	KU171706	KU171686
F. pseudograminearum	NRRL 28062^{HT}	Unknown	Unknown	MW233090	JX171637	JX171524
F. sambucinum	MAFF 150447	Squash	Japan	LC637559	LC637561	–
	CBS 146.95^{HT}	*Solanum tuberosum*	United Kingdom	KM231941	KM232381	–
F. sibiricum	NRRL 53432	Oat	Russia	HM744686	HQ154474	–
	NRRL 53430	Oat	Russia	HM744684	MW233474	MW233302
F. sporotrichioides	CBS 131779	*Avena sativa*	Canada	JX119003	JX162545	–
F. transvaalense	LLC3337	Soil	Australia	OP487291	OP486855	OP486422
	NRRL 31008	Soil	Australia	MW233102	MW233446	MW233274
F. venenatum	CBS 458.93^{T}	*Winter wheat*	Australia	KM231942	KM232382	–
	NRRL 25413	Unknown	United Kingdom	MW233080	MW233423	MW233251
***F. solani* species complex**						
F. ambrosium	NRRL 22346	*Euwallacea fornicatus*	India	FJ240350	EU329503	KC691587
	NRRL 20438	*Euwallacea fornicatus*	India	AF178332	JX171584	JX171470
F. bataticola	CBS 144397	*Ipomoea batatas*	USA	AF178343	EU329509	MW218099
	CBS 144398^{T}	*Ipomoea batatas*	USA	AF178344	FJ240381	MW218100
F. borneense	CBS 145462	Bark or recently dead tree	Indonesia	AF178352	EU329515	MW834213
F. breviconum	CBS 203.31	Twig	Philippines	LR583599	LR583820	MW218103
F. cicatricum (Outgroup)	CBS 125552	Dead twig	Slovenia	HM626644	HQ728153	–
F. cryptoseptatum	CBS 145463^{T}	Bark	French Guiana	AF178351	EU329510	MW834215
F. cucurbiticola	CBS 410.62	*Cucurbita viciifolia*	Netherlands	DQ247640	LR583824	MW834216
	CBS 616.66^{T}	*Cucurbita viciifolia*	Netherlands	DQ247592	LR583825	MW834217

Species name	Culture/specimen[1]	Host	Country/area	GenBank/ENA accession number[2]		
				TEF–1α	RPB2	RPB1
F. euwallaceae	CBS 135854^{T}	*Euwallacea* sp. on *Persea americana*	Israel	JQ038007	JQ038028	JQ038021
	NRRL 62626	*Euwallacea* sp. on *Persea americana*	USA	KC691532	KU171702	KU171682
F. haematococcum	CBS 119600^{ET}	Dying tree	Sri Lanka	DQ247510	LT960561	–
F. helgardnirenbergiae	CBS 145469^{T}	Bark	French Guiana	AF178339	EU329505	–
F. hunanense	HN33-8-2 *	Chinese fir	China	ON734393	ON734373	OR683272
	HN33-8-2-1 *	Chinese fir	China	ON734394	ON734374	OR683273
	HN33-8-2-2 *	Chinese fir	China	ON734395	ON734375	OR683274
	HN33-8-2-3 *	Chinese fir	China	ON734396	ON734376	OR683275
F. illudens	NRRL 22090	*Beilschmiedia tawa*	New Zealand	AF178326	JX171601	JX171488
F. kuroshium	CBS 142642^{T}	*Euwallacea* sp. on *Platanus racemosa*	USA	KX262216	LR583837	MW834227
F. kurunegalense	CBS 119599^{T}	Recently cut tree	Sri Lanka	DQ247511	LR583838	MW834228
F. lichenicola	CBS 279.34^{T}	Human	Somalia	LR583615	LR583840	–
F. mahasenii	CBS 119594^{T}	Dead branch on live tree	Sri Lanka	DQ247513	LT960563	MW834231
F. neocosmosporiellum	CBS 446.93^{T}	Soil	Japan	LR583670	LR583898	MW834257
F. oligoseptatum	CBS 143241^{T}	*Euwallacea validus* on *Ailanthus altissima*	USA	KC691538	LR583854	–
	NRRL 62578	*Euwallacea validus* on *Ailanthus altissima*	USA	KC691537	KC691626	KC691595
F. phaseoli	NRRL 31041^{T}	*Glycine max*	USA	AY220193	JX171643	JX171530
F. piperis	CBS 145470^{T}	*Piper nigrum*	Brazil	AF178360	EU329513	MW834241
F. plagianthi	NRRL 22632	*Hoheria glabrata*	New Zealand	AF178354	JX171614	JX171501
F. protoensiforme	CBS 145471^{T}	Dicot tree	Venezuela	AF178334	EU329498	MW834244
F. pseudensiforme	CBS 130.78	*Cocos nucifera*	Indonesia	DQ247635	LR583868	MW834245
	CBS 125729^{T}	Dead tree	Sri Lanka	KC691555	KC691645	KC691615
F. rectiphorum	CBS 125727^{T}	Dead tree	Sri Lanka	DQ247509	LR583871	MW834249
F. samuelsii	CBS 114067^{T}	Bark	Guyana	LR583644	LR583874	MW834252
F. staphyleae (Outgroup)	NRRL 22316	*Staphylea trifolia*	USA	AF178361	EU329502	JX171496
Fusarium sp.	YZU 171871	*Citrus sinensis*	China	MK370098	MK370099	–
	YZU 171870	*Citrus sinensis*	China	MH423886	MH423885	–
F. venezuelense	CBS 145473^{T}	Bark	Venezuela	AF178341	EU329507	–
F. xiangyunensis	ZF-2018	Soil	China	MH992629	–	–
F. yamamotoi	CBS 144395	*Xanthoxylum piperitum* branch	Japan	AF178328	EU329496	MW218112
	CBS 144396^{ET}	*Xanthoxylum piperitum* trunk	Japan	AF178336	FJ240380	MW218113

[1] BBA: Biologische Bundesanstalt für Land- und Forstwirtschaft, Institut für Mikrobiologie, Berlin, Germany; CBS: Westerdijk Fungal Biodiverity Institute (WI), Utrecht, The Netherlands; CPC: Collection of P.W. Crous, held at WI; HMAS: Herbarium Mycologicum Academiae Sinicae, Chinese Academy of Sciences, Beijing, China; NRRL: Agricultural Research Service Culture Collection, National Center for Agricultural Utilization Research, USDA, Peoria, IL, USA; URM: the University Recife Mycology culture collection at the Universidade Federal de Pernambuco, Recife, Brazil; FCCUFG: Fungal Culture Collection of the Universidade Federal de Goiás; FRC: Fusarium Research Center, University Park, PA, USA; MUCL: Mycotheque de lUniversite Catholique de Louvain, Louvain-la-Neuve, Belgium; ^{ET}: Ex-epitype, ^{LT}: Ex-lectotype, ^{NT}: Ex-neotype, ^{HT}: Ex-holotype, ^{T}: Ex-type, *: Sequences generated in this study.
[2] TEF-1α: translation elongation factor 1-alpha; RPB2: RNA polymerase second largest subunit; RPB1: RNA polymerase largest subunit.

Phylogenetic analyses

The sequences generated in this study were compared against nucleotide sequences in GenBank using BLAST to determine closely related taxa. Alignments of different loci, including the sequences obtained from this study and sequences downloaded from the GenBank, were initially performed with the MAFFT v.7 online server (https://mafft.cbrc.jp/alignment/server/) (Katoh and

Standley 2013) and then manually adjusted in MEGA v. 10 (Kumar et al. 2018). The post-alignment sequences of multiple loci were concatenated in PhyloSuite software (Zhang et al. 2020). Maximum Likelihood (ML) and Bayesian Inference (BI) analyses were conducted with PhyloSuite software using IQ-TREE ver. 1.6.8 (Nguyen et al. 2015) and MrBayes v. 3.2.6 (Ronquist et al. 2012), respectively. ModelFinder was used to carry out statistical selection of best-fit models of nucleotide substitution using the corrected Akaike information criterion (AIC) (Kalyaanamoorthy et al. 2017) (Suppl. material 1: table S3). For ML analyses the default parameters were used and bootstrap support (BS) was carried out using the rapid bootstrapping algorithm with the automatic halt option. Bayesian analyses included two parallel runs of 2,000,000 generations, with the stop rule option and a sampling frequency set to each 1,000 generations. The 50% majority rule consensus trees and posterior probability (PP) values were calculated after discarding the first 25% of the samples as burn-in. Phylogenetic trees were visualized in FigTree v. 1.4.2 (http://tree.bio.ed.ac.uk/software/figtree/) (Rambaut 2014).

Phylogenetically related but ambiguous species were analyzed using the genealogical concordance phylogenetic species recognition (GCPSR) model by performing a pairwise homoplasy index (PHI) test as described by Quaedvlieg et al. (2014). The PHI test was performed in SplitsTree4 (Huson 1998; Huson and Bryant 2006) in order to determine the recombination level within phylogenetically closely related species using a concatenated multi-locus dataset (*TEF-1α*, *RPB2* and *RPB1*). If the pairwise homoplasy index results were below a 0.05 threshold ($\Phi_w < 0.05$), it indicates significant recombination present in the dataset. The relationship among the closely related species was visualized by constructing splits graphs.

Morphological study

One representative isolate was randomly selected from each *Fusarium* species for morphological research according to the method of Leslie and Summerell (2006). The isolates were transferred from the actively growing edge of a 4-day old colony by cutting mycelial blocks (6 mm in diameter), plated on to fresh potato dextrose agar (PDA) (Crous et al. 2021), oatmeal agar (OMA) (Crous et al. 2021), corn meal agar (CMA) (Thompson et al. 2013), and synthetic nutrient-poor agar (SNA) (Crous et al. 2021) plates and incubated at 25 °C in the dark. Alternatively, the isolates were also plated on to carnation leaf agar (CLA) (Crous et al. 2021) to induce sporulation when this failed on other media. The growth rate was recorded by measuring the diameter of the colonies until day 5, and the mean growth rate was calculated per day. The colony characters including colony color, texture, and pigment production were also recorded. The morphology and size of ascomata and conidiomata were studied and recorded using a Zeiss stereo microscope (SteRo Discovery v20). The shape, color and size of conidiophores, conidia were observed using a ZEISS Axio Imager A2m microscope (ZEISS, Germany) with differential interference contrast (DIC) optics. At least 30 measurements per structure were performed using Carl Zeiss Axio Vision software to determine their sizes, unless no or fewer individual structures were produced.

Pathogenicity tests

The fungal isolates HN43-17-1, SJ1-10, LC14, GZ7-20-1, and HN33-8-2 were randomly selected from the *Fusarium* species for Koch's postulates test. A conidial suspension of 10^6 conidia/ml of each isolate was used for inoculation.

For *in vitro* inoculation, healthy young leaves of *C. lanceolata* were collected from 1-year-old *C. lanceolata* plants on the campus of Nanjing Forestry University, Jiangsu, China. Detached leaves were surface-sterilized with 75% ethanol, washed three times with sterile water, and air-dried on sterile filter paper. A 10 µl aliquot of conidial suspension was transferred to a sterile plastic tube (6 mm diameter, 20 mm deep), in which a leaf was placed so that the base of the leaf was immersed in the conidial suspension. The control was treated with the same amount of double-distilled water. Leaves in the tubes were then put in plastic trays (40 × 25 cm), covered with a piece of plastic wrap to maintain relative humidity at 99%, and incubated at 25 °C in the dark for 5 days. Each treatment had eight replicates, and the experiment was conducted three times. Symptom development on the detached leaves was evaluated by determining the means of lesion lengths at 5 days post inoculation (dpi). The data were analyzed by analysis of variance (ANOVA) using SPSS v. 18 software. LSD's range test was used to determine significant differences among or between different treatments (Chung et al. 2020). Origin v. 8.0 software was used to draw histograms (Li et al. 2020).

For *in vivo* inoculation, shoots from *C. lanceolata* tissue culture seedlings provided by Fujian Yangkou Forest Farm, Fujian, China were used. Fifty-four bottles of seedlings (cultured with 0.6% water agar medium, one seedling per bottle) were prepared. A 10 µl aliquot of conidial suspension was applied onto each of the leader shoots. The same volume of distilled water was used as a control. After inoculation, the seedlings were incubated at 28 °C with a 12-h/12-h light/dark photoperiod for 10 days. The experiment was conducted three times, and each treatment had three replicates. Pathogens were re-isolated from the resulting lesions and identified as afore-described.

Results

Phylogenetic analyses

A total of 20 *Fusarium* isolates were isolated from the diseased *C. lanceolata* samples showing the symptom of leaf blight and used for phylogenetic analyses. Three-locus phylogenetic analysis used 37 isolates of 22 related taxa from the *F. fujikuroi* species complex. *Fusarium zealandicum* CBS 111.93 (ex-type) was used as the out-group. A total of 2219 characters (*RPB1*: 1-901, *RPB2*: 902-1692, *TEF-1α*: 1693-2219) were included in the phylogenetic analyses. The Bayesian Inference (BI) and Maximum-likelihood (ML) phylogenetic analyses of the isolates of *F. fujikuroi* species complex produced topologically similar trees. The BI posterior probabilities (PP) were plotted on the ML tree (Fig. 1). In the combined analyses, four isolates (SJ1-10, SJ1-10-1, SJ1-10-2, and SJ1-10-3) were placed in the same clade with *F. concentricum* with high support (ML-BS/BI-PP = 100/1). Four isolates (HN43-17-1, HN43-17-1-1, HN43-17-1-2, and HN43-17-1-3) clustered in *F. fujikuroi* clade with high supports (ML-BS/BI-PP = 100/1).

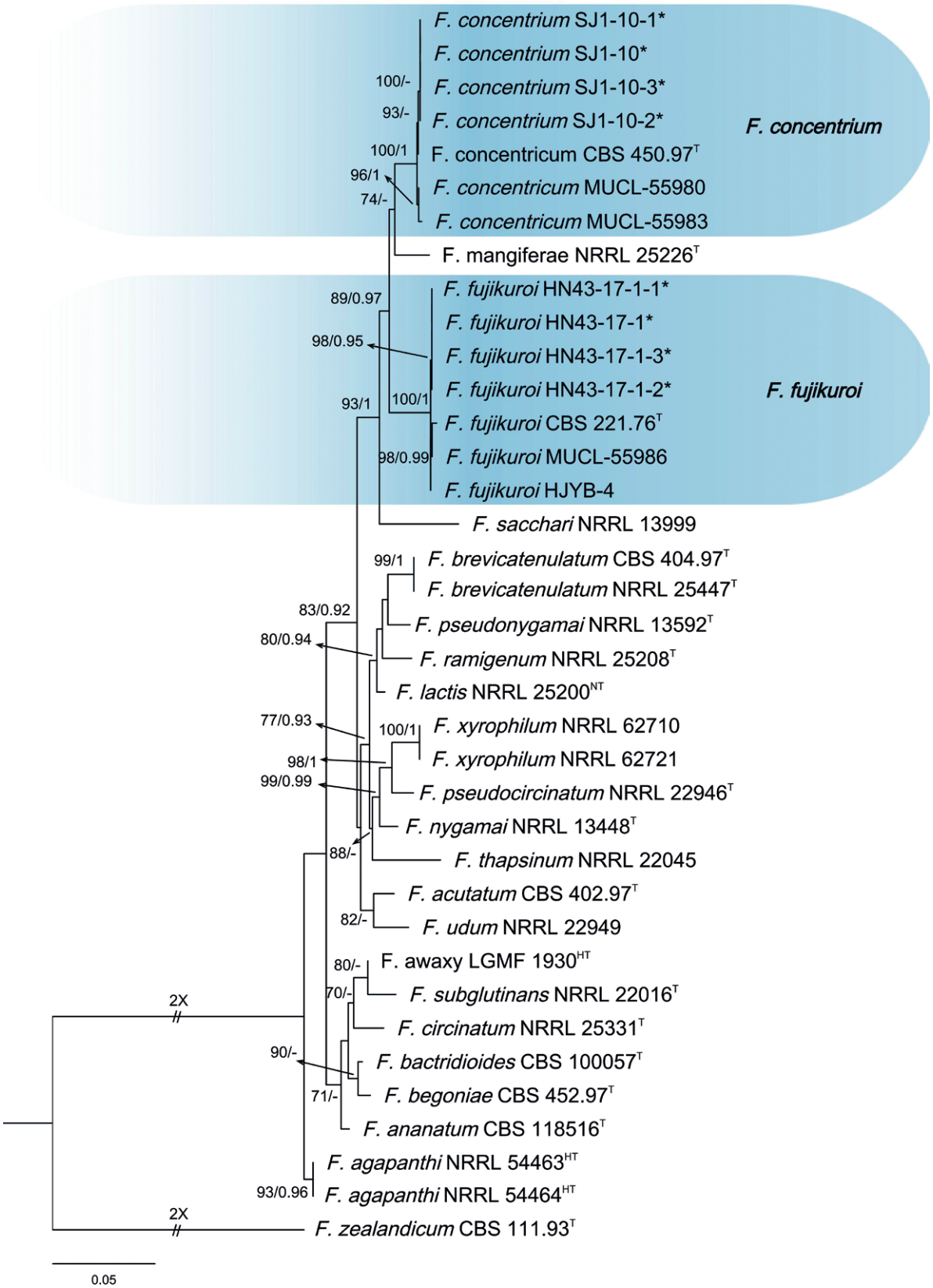

Figure 1. Phylogenetic relationships of 37 isolates of the *Fusarium fujikuroi* species complex with related taxa derived from concatenated sequences of the *TEF-1α*, *RPB2*, and *RPB1* genes/region using Bayesian inference (BI) and maximum likelihood (ML) methods. Bootstrap support values from ML ≥ 70% and BI posterior values ≥ 0.9 are shown at nodes (ML/BI). *Fusarium zealandicum* CBS 111.93^{T} was the outgroup. * indicates strains of this study. ^{T} indicates ex-types or ex-epitypes. ^{LT}: Ex-lectotype, ^{NT}: Ex-neotype, ^{HT}: Ex-holotype.

The three-locus phylogenetic analysis used 16 isolates of 8 related taxa from the *F. lateritium* species complex. *Fusarium sublunatum* CBS 189.34 (ex-type) was used as the out-group. A total of 2063 characters (*RPB1*: 1-615, *RPB2*: 616-1391, *TEF-1α*: 1392-2063) were included in the phylogenetic analyses. The Bayesian Inference (BI) and Maximum-likelihood (ML) phylogenetic analyses of the isolates of *F. lateritium* species complex produced topologically similar trees. The BI posterior probabilities (PP) were plotted on the ML tree (Fig. 2). Phylogenetic analyses showed that the four isolates (LC14, LC14-1, LC14-2, and LC14-3) clustered in a distinct clade with high supports (ML-BS/BI-PP = 97/0.99), which was distinct from all other known species and closely related to *F. citri-sinensis* (ex-type, YZU 191316), *F. cassiae* (ex-holotype, MFLUCC 18-0573), *F. stilboides* (ex-type, CBS 746.79) (Fig. 2). When applying the GCPSR concept to these isolates, the concatenated sequence dataset of three-loci (*TEF-1α*, *RPB2*, and *RPB1*) was subjected to the PHI test showed that no significant recombination was detected among these isolates/taxa (Φ_w = 0.2461) (Fig. 3A), which was a solid support for the proposition that these isolates belonged to four distinct taxa.

The three-locus phylogenetic analysis used 41 isolates of 29 related taxa from the *F. solani* species complex. *Fusarium staphyleae* NRRL 22316 and

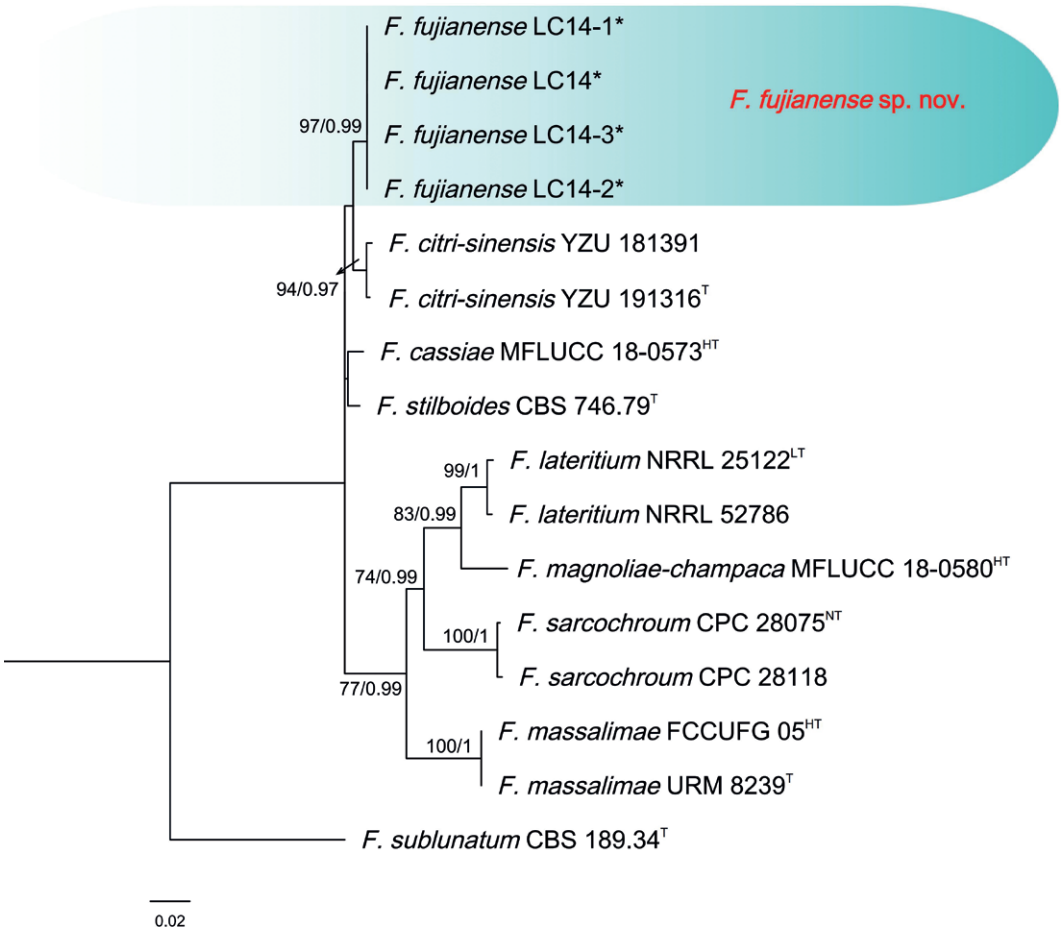

Figure 2. Phylogenetic relationships of 16 isolates of the *Fusarium lateritium* species complex with related taxa with concatenated sequences of the *TEF-1α*, *RPB2*, and *RPB1* loci using Bayesian inference (BI) and maximum likelihood (ML) methods. Bootstrap support values from ML ≥ 70% and BI posterior values ≥ 0.9 are shown at nodes (ML/BI). *Fusarium sublunatum* CBS 189.34^T was the outgroup. * indicates strains of this study. ^{T} indicates the ex-type strains. ^{LT}: Ex-lectotype, ^{NT}: Ex-neotype, ^{HT}: Ex-holotype.

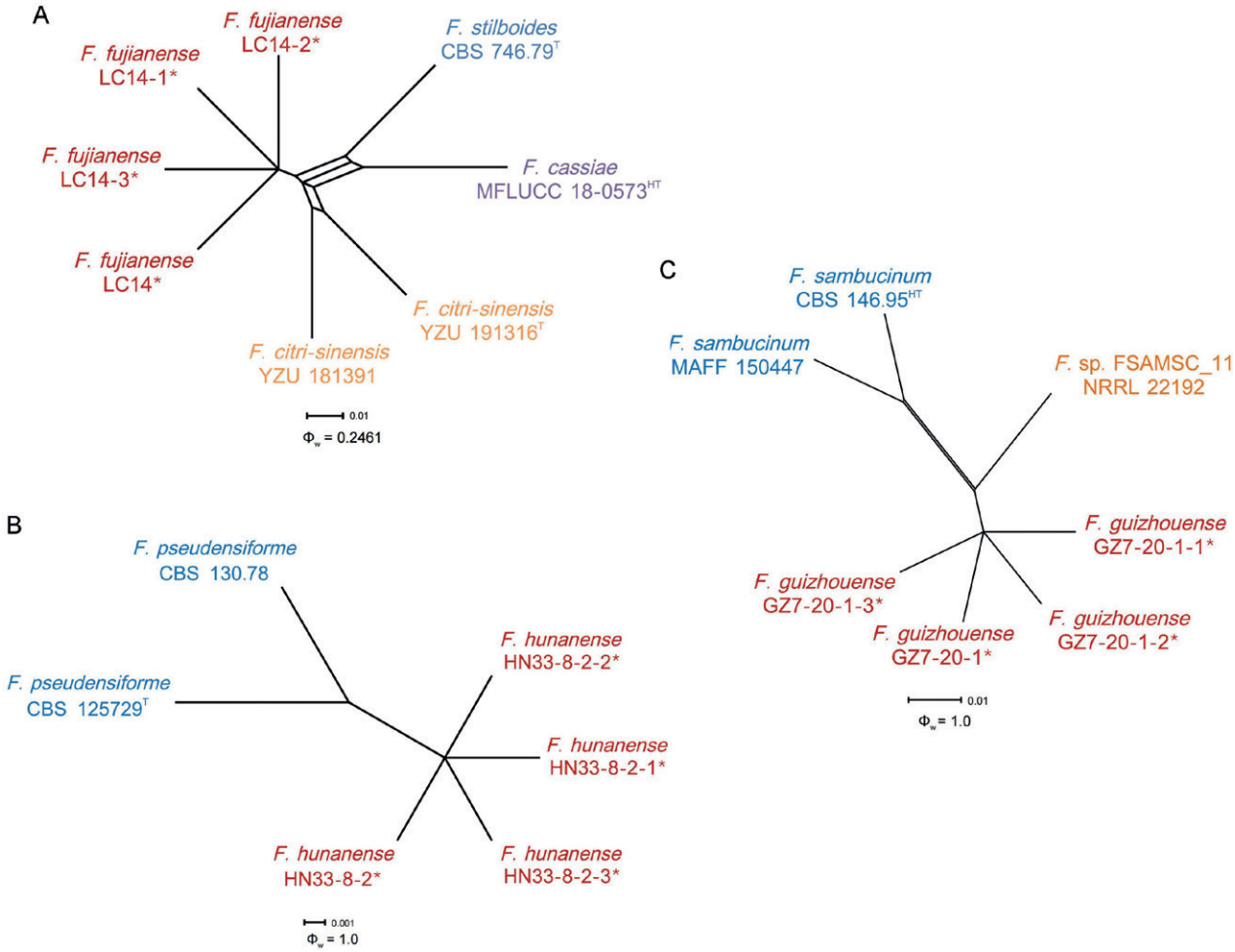

Figure 3. Splitgraphs showing the results of the pairwise homoplasy index (PHI) test of three newly described taxa and closely related species using both LogDet transformation and splits decomposition **A** the PHI of *Fusarium fujianense* sp. nov. with their phylogenetically related isolates or species **B** the PHI of *F. hunanense* sp. nov. with their phylogenetically related isolates or species **C** the PHI of *F. guizhouense* sp. nov. with their phylogenetically related isolates or species. PHI test value (Φ_w) < 0.05 indicate significant recombination within a dataset. * indicates isolates of this study. ^{T} indicates ex-types. ^{HT} indicates ex-holotypes.

F. cicatricum CBS 125552 were used as the out-group. A total of 2023 characters (*RPB1*: 1-640, *RPB2*: 641-1440, *TEF-1α*: 1441-2023) were included in the phylogenetic analyses. The Bayesian Inference (BI) and Maximum-likelihood (ML) phylogenetic analyses of the isolates of *F. solani* species complex produced topologically similar trees. The BI posterior probabilities (PP) were plotted on the ML tree (Fig. 4). Phylogenetic analyses showed that the four isolates (HN33-8-2, HN33-8-2-1, HN33-8-2-2, and HN33-8-2-3) clustered in a distinct clade with high supports (ML-BS/BI-PP = 100/1). These isolates were distinct from all other known species and closely related to *F. pseudensiforme* (ex-type, CBS 125729) (Fig. 4). When applying the GCPSR concept to this species, the concatenated sequence dataset of three-loci (*TEF-1α*, *RPB2*, and *RPB1*) was subjected to the PHI test showed that no significant recombination was detected among these isolates/taxa (Φw = 1.0) (Fig. 3B), which was a good support for the proposition that these isolates belonged to two distinct taxa.

The three-locus phylogenetic analysis used 30 isolates of 18 related taxa from the *F. sambucinum* species complex. *Fusarium concentricum* CBS 450.97

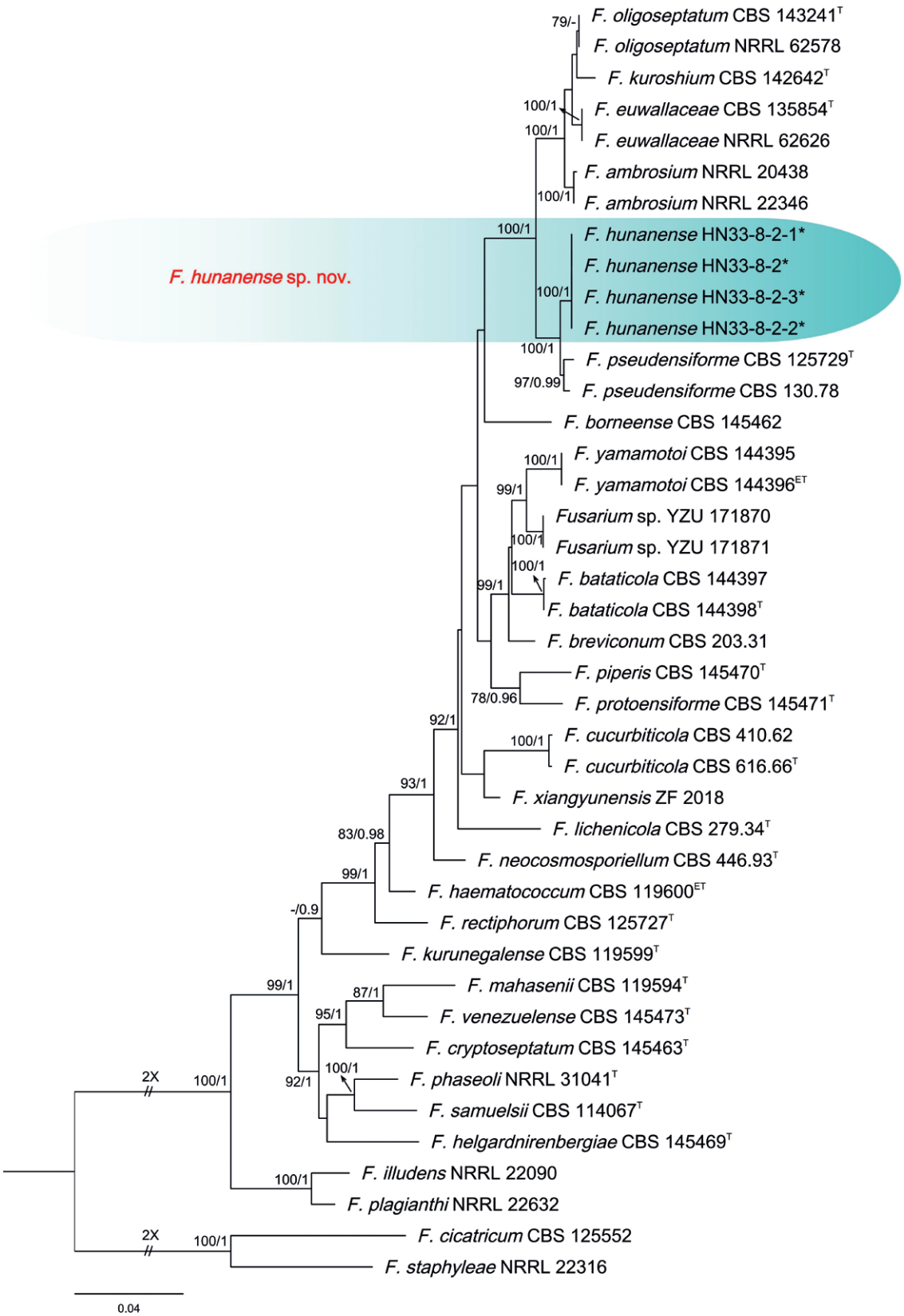

Figure 4. Phylogenetic relationships of 41 isolates of the *Fusarium solani* species complex with related taxa with concatenated sequences of the *TEF-1α*, *RPB2*, and *RPB1* loci using Bayesian inference (BI) and maximum likelihood (ML) methods. Bootstrap support values from ML ≥ 70% and BI posterior values ≥ 0.9 are shown at nodes (ML/BI). *Fusarium staphyleae* NRRL 22316 and *F. cicatricum* CBS 125552 were the outgroup. * indicates strains of this study. T indicates the ex-type strains. ET indicates ex-epitypes.

(ex-type) was used as the out-group. A total of 2115 characters (*RPB1*: 1-641, *RPB2*: 642-1538, *TEF-1α*: 1539-2115) were included in the phylogenetic analyses. The Bayesian Inference (BI) and Maximum-likelihood (ML) phylogenetic analyses of the isolates of *F. sambucinum* species complex produced topologically similar trees. The BI posterior probabilities (PP) were plotted on the ML tree (Fig. 5). Phylogenetic analyses showed that the four isolates (GZ7-20-1, GZ7-20-1-1, GZ7-20-1-2, and GZ7-20-1-3) clustered in a distinct clade with high supports (ML-BS/BI-PP = 100/1), which was distinct from all other known species and identified as closely related to *F. venenatum* (ex-type, CBS 458.93), *F. poae* (ex-type, NRRL 26941), and *F. sambucinum* (ex-holotype, CBS 146.95) (Fig. 5). When applying the GCPSR concept to these isolates, the concatenated sequence dataset of three-loci (*TEF-1α*, *RPB2*, and *RPB1*) was subjected to the PHI test and showed that no significant recombination was detected among these isolates/taxa (Φ_w = 0.7313) (Fig. 3C). The split tree decomposition network of these multiple combinations was clearly detected within four separate groups.

Taxonomy

The results of the molecular analyses and observations of morphological characteristics in culture indicated that the 20 isolates from *C. lanceolata* belonged to five *Fusarium* species, among which two were known taxa (*F. concentricum* and *F. fujikuroi*) and three were new to science (*F. fujianense*, *F. guizhouense*, and *F. hunanense*). This study selected the representative strains of each *Fusarium* species SJ1-10 (*F. concentricum*), LC14 (*F. fujianense*), HN43-17-1 (*F. fujikuroi*), GZ7-20-1 (*F. guizhouense*), and HN33-8-2 (*F. hunanense*) for detailed morphological characterization.

Fusarium concentricum **Nirenberg & O'Donnell, Mycologia 90 (3): 442 (1998)**
MycoBank No: 444884
Suppl. material 1: fig. S1

Description. Sexual state not observed. Asexual state: sporulation abundant from sporodochia, rarely from conidiophores formed directly on the substrate mycelium. Conidiophores in the aerial mycelium branched, bearing terminal or intercalary monophialides, often reduced to single phialides. Phialides subulate to subcylindrical, smooth, thin-walled, (2.3–)4.9–15.5(–18.3) × (1.1–)1.4–2.8(–3.5) µm, (mean ± SD = 10.2 ± 5.3 × 2.1 ± 0.7 µm, n = 9), without periclinal thickening. Microconidia in the aerial mycelium hyaline, ellipsoidal to falcate, smooth, thin-walled, 0–1-septate, (3.8–)5.9–9.1(–11.3) × (1.9–)2.5–3.4(–4.3) µm (mean ± SD = 7.5 ± 1.6 × 3.0 ± 0.5 µm, n = 60), forming small false heads on the tips of monophialides. Sporodochia pale orange colored, formed abundantly on carnation leaves. Conidiophores in sporodochia (27.7–)40.6–49.8(–51.7) µm, (mean ± SD = 45.2 ± 4.6 µm, n = 35), verticillately branched and densely packed, bearing apical whorls of 2–3 monophialides or rarely single lateral monophialides; sporodochial phialides subulate to subcylindrical, (9.5–)11.4–16.5(–20.4) × (2.2–)2.7–4.0(–4.7) µm, (mean ± SD = 13.9 ± 2.5 × 3.4 ± 0.6 µm, n = 45), smooth, thin-walled. Sporodochial macroconidia falcate, curved dorsiventrally with almost parallel sides tapering slightly towards both ends, with

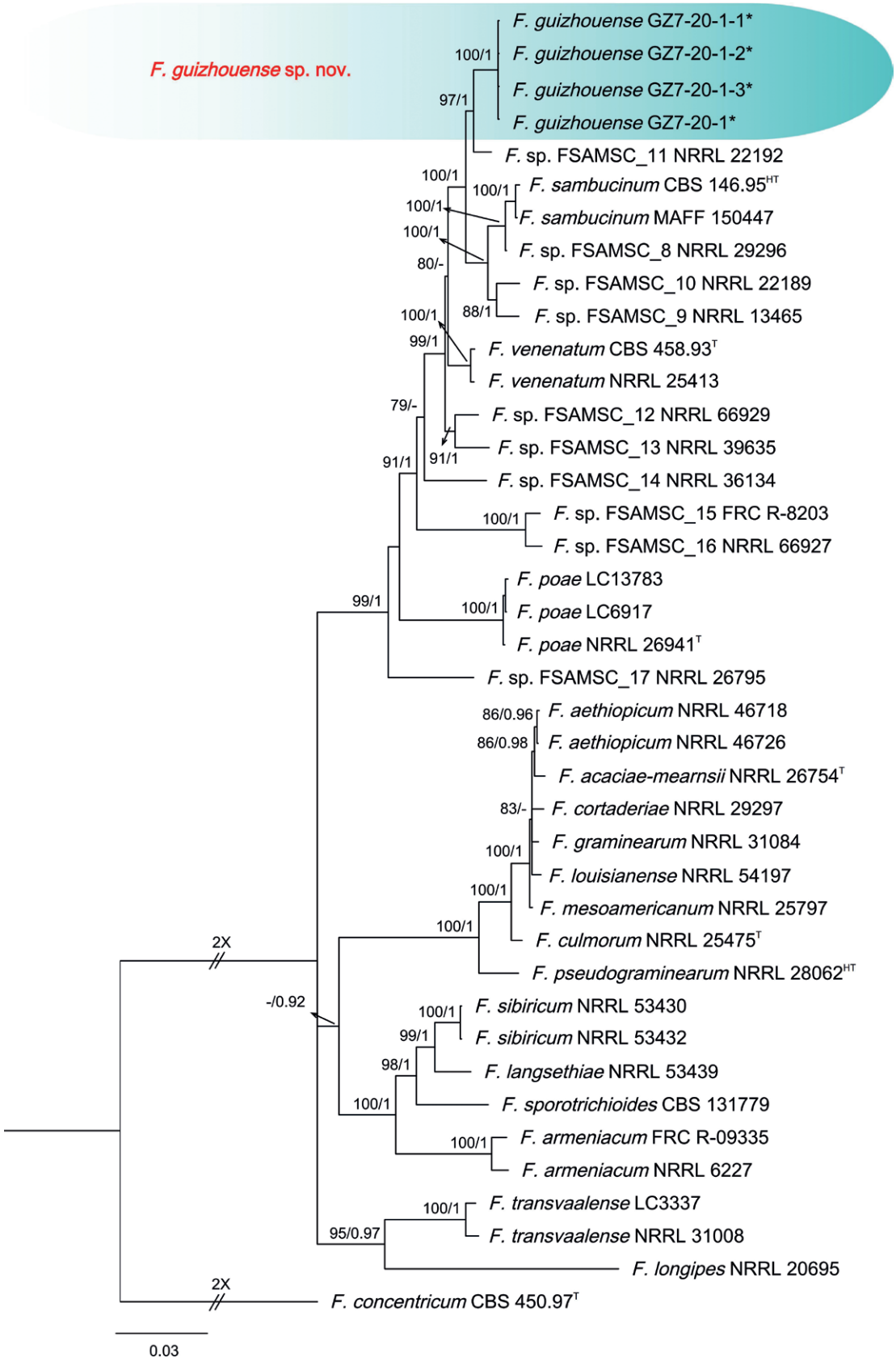

Figure 5. Phylogenetic relationships of 30 isolates of the *Fusarium sambucinum* species complex with related taxa with concatenated sequences of the *TEF-1α*, *RPB2*, and *RPB1* loci using Bayesian inference (BI) and maximum likelihood (ML) methods. Bootstrap support values from ML ≥ 70% and BI posterior values ≥ 0.9 are shown at nodes (ML/BI). *F. concentricum* CBS 450.97^{T} was the outgroup. * indicates strains of this study. ^{T} indicates the ex-type strains. ^{HT} indicates ex-holotypes.

a blunt to papillate, curved apical cell and a foot cell, 3-septate, (23.2–)30.2–40.5(–43.7) × (3.4–)3.9–4.9(–5.5) µm, (mean ± SD = 35.3 ± 5.2 × 4.4 ± 0.5 µm, n = 60), 4-septate, (35.5–)38.0–48.8(–49.4) × (3.4–)3.4–4.3(–4.4) µm, (mean ± SD = 43.4 ± 5.4 × 3.9 ± 0.4 µm, n = 10), 5-septate, (49.5–)49.7–57.2(–59.1) × (3.5–)3.6–4.2(–4.2) µm, (mean ± SD = 53.4 ± 3.6 × 3.9 ± 0.3 µm, n = 10), hyaline, thin- and smooth-walled. Chlamydospores absent.

Culture characteristics. Colonies on PDA growing in the dark with an average growth rate of 9.3 mm/d at 25 °C. Colony surface white to pale purple, flat or slightly raised at the center; colony margins irregular, filiform. Reverse light yellow. Odor absent. Colonies on SNA incubated at 25 °C in the dark were regular, round, aerial mycelium absent or scant, growing at 13.1 mm/d. Colonies on OMA incubated at 25 °C in the dark were regular, round, aerial mycelium abundant, loose to densely floccose, growing at 13.2 mm/d. Reverse light purple. Colonies on CMA incubated at 25 °C in the dark were regular, round, colony surface and reverse pale gray at the center, aerial mycelium absent or scarce, growing at 11.9 mm/d.

Materials examined. China, Guangxi Zhuang Autonomous Region, Liuzhou City, Sanjiang Dong Autonomous County, Guyi Town, 25°25'48"N, 109°28'47"E, isolated from leaf spots of *Cunninghamia lanceolata*, May 2017, Wen-Li Cui, isolates: SJ1-10, SJ1-10-1, SJ1-10-2, SJ1-10-3.

Notes. The isolate SJ1-10 in this study was in the same clade with *F. concentricum* CBS 450.97 (ex-type). Morphologically, 0-septate microconidia (3.8–11.3 × 1.9–4.3 µm) of the isolate SJ1-10 were similar with the 0-septate microconidia (7.0–12.2 ×2.3–3.9 µm) of the ex-type (CBS 450.97) of *F. concentricum* (Nirenberg and O'Donnell 1998). Five-septate macroconidia (49.5–59.1 × 3.5–4.2 µm) of the isolate SJ1-10 were similar with the 5-septate macroconidia (49.0–64.8 × 3.6–4.0 µm) of the ex-type (CBS 450.97) of *F. concentricum* (Nirenberg and O'Donnell 1998).

Fusarium fujikuroi Nirenberg, Mitteilungen der Biologischen Bundesanstalt für Land- und Forstwirtschaft 169: 32 (1976)

MycoBank No: 314213

Suppl. material 1: fig. S2

Description. Sexual state not observed. Asexual state: Sporulation abundant from sporodochia, rarely from conidiophores formed directly on the substrate mycelium. Conidiophores in the aerial mycelium branched, bearing terminal or intercalary phialides. Phialides subulate to subcylindrical, smooth, thin-walled, (11.5–)14.7–22.9(–30.0) µm × (1.8–)2.0–3.6(–4.0) µm, (mean ± SD = 18.8 ± 4.1 µm × 2.8 ± 0.8 µm, n = 37), without periclinal thickening; microconidia hyaline, short clavate to cylindrical, slender to relatively straight, smooth, thin-walled, 0-septate, (5.4–)6.7–11.3(–15.5) × (2.0–)2.5–3.5(–4.4) µm, (mean ± SD = 9.0 ± 2.3 × 3.0 ± 0.5 µm, n = 81), forming small false heads on the tips of phialides. Chlamydospores formed occasionally, mostly in pairs or chains, terminal or intercalary, globose to subglobose, smooth-walled, (6.0–)6.2–8.0(–8.3) × (4.4–)4.4–5.2(–5.6) µm, (mean ± SD = 7.1 ± 0.9 × 4.8 ± 0.4 µm, n = 6). Sporodochia and macroconidia not observed.

Culture characteristics. Colonies on PDA growing in the dark with an average growth rate of 13.9 mm/d at 25 °C. Colony surface white to purple, flat or slight-

ly raised at the center; colony round, regular, margins filiform, aerial mycelium abundant. Reverse purple with white periphery. Odor absent. Colonies on SNA incubated at 25 °C in the dark were regular, round, growing at 8.1 mm/d. Colony surface pure white, aerial mycelium absent or scant. Reverse pure white, without diffusible pigments. Colonies on OMA incubated at 25 °C in the dark were regular, round, aerial mycelium abundant, loose to densely floccose, growing at 12.5 mm/d. Colony white to dark purple and with white to dark violet pigmentation. Colonies on CMA incubated at 25 °C in the dark were regular, round, colony surface and reverse white, aerial mycelium absent or scant, growing at 11.3 mm/d.

Materials examined. China, Hunan province, Yiyang City, Heshan District, Henglongqiao Town, 28°27'24"N, 112°29'7"E, isolated from leaf spots of *Cunninghamia lanceolata*, May 2017, Wen-Li Cui, isolates: HN43-17-1, HN43-17-1-1, HN43-17-1-2, HN43-17-1-3.

Notes. The isolate HN43-17-1 in this study was in the same clade with *F. fujikuroi* CBS 221.76 (ex-type). Morphologically, 0-septate microconidia, (5.4–15.5 × 2–4.4 µm) of the isolate HN43-17-1 were more variable than the 0-septate microconidia (12.2–12.9 × 3.4–3.7 µm) of the ex-type (CBS 221.76) of *F. fujikuroi* (Ibrahim et al. 2016).

Fusarium fujianense **Lin Huang, Jiao He & D.W. Li, sp. nov.**

Index Fungorum Number: IF900473

Fig. 6

Etymology. Epithet is after Fujian province where the type specimen was collected.

Holotype. China, Fujian Province, Nanping City, Shunchang County, Yangkou Forest Farm, 26°48'36"N, 117°52'48"E, isolated from leaf spots of *Cunninghamia lanceolata*, May 2017, Wen-Li Cui, (holotype: CFCC 57576). Holotype specimen is a living specimen being maintained via lyophilization at the China Forestry Culture Collection Center (CFCC). Ex-type (LC14) is maintained at the Forest Pathology Laboratory, Nanjing Forestry University.

Host/distribution. From *C. lanceolata* in Yangkou Forest Farm, Shunchang County, Nanping City, Fujian Province, China.

Description. Sexual state not observed. Asexual state: Sporulation abundant from sporodochia, rarely from conidiophores formed directly on the substrate mycelium. Conidiophores in the aerial mycelium unbranched, bearing terminal or intercalary monophialides, often reduced to single phialides. Phialides subulate to subcylindrical, smooth, thin-walled, (9.2–)10.3–16.3(–18.0) µm × (2.5–)2.6–3.4(–3.6) µm, (mean ± SD = 13.3 ± 3.0 µm × 3.0 ± 0.4 µm, n = 11), without periclinal thickening; microconidia subcylindrical to clavate, hyaline, smooth- and thin-walled, 0-septate, (5.6–)6.0–8.2(–8.3) µm × (1.9–)2.1–2.5(–2.7) µm, (mean ± SD = 7.1 ± 1.1 µm × 2.3 ± 0.2 µm, n=11), forming small false heads on the tips of monophialides. Sporodochia pale orange colored, formed abundantly on PDA after 40 days. Conidiophores in sporodochia (9.7–)18.8–31.5(–37.9) µm, (mean ± SD = 25.1 ± 6.4 µm, n = 37), irregularly branched and densely packed, bearing apical whorls of monophialides or 2–3 ployphialides; sporodochial phialides subulate to subcylindrical, (5.6–)10.0–16.1(–18.8) × (1.4–)2.5–3.9(–4.8) µm, (mean ± SD = 12.7 ± 3.4 × 3.2 ± 0.7 µm, n = 39), smooth, thin-walled. Sporodochial mesoconidia falcate, curved dorsiventrally with almost parallel sides ta-

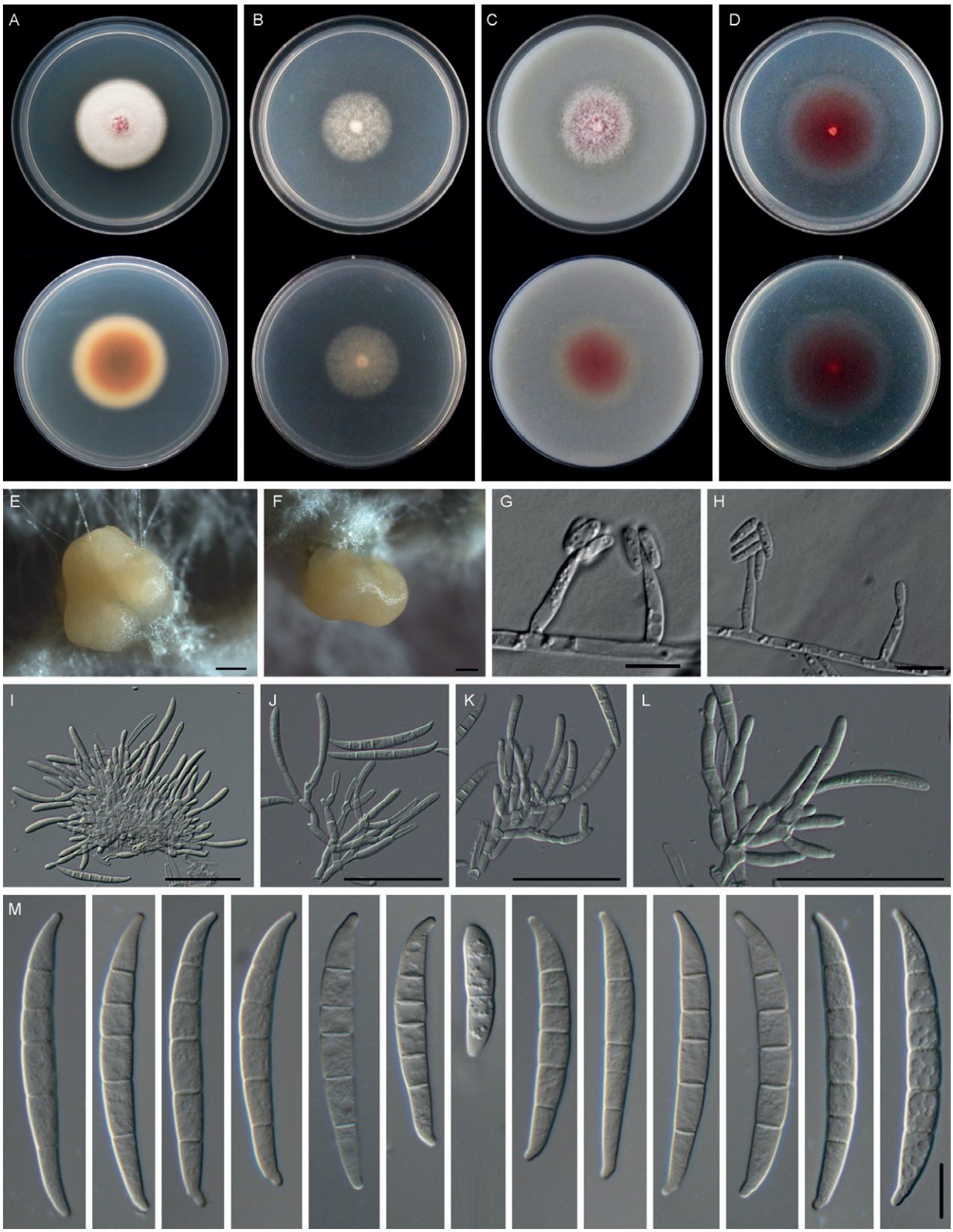

Figure 6. *Fusarium fujianense* (LC14) **A–D** colonies on PDA, SNA, OMA, and CMA, respectively, after 5 days at 24 °C in the dark **E, F** sporodochia formed on PDA **G, H** aerial conidiophores, phialides, and microconidia **I–L** sporodochial conidiophores, phialides, and macroconidia **M** mesoconidium (1-septate) and macroconidia (4–6-septate). Scale bars: 200 µm (**E, F**); 10 µm (**G–M**).

pering slightly towards both ends, with a blunt to papillate, curved apical cell and a foot-like basal cell, 1-septate, (21.8–)22.0–23.6(–23.8) × (4.7–)4.9–5.3(–5.3) µm, (mean ± SD = 22.8 ± 0.8 × 5.1 ± 0.2 µm, n = 6), macroconidia 4–6-septate, (40.2–)45.9–59.1(–63.4) × (4.5–)4.8–5.8(–6.9) µm, (mean ± SD = 52.5 ± 6.6 × 5.3 ± 0.5 µm, n = 18), hyaline, smooth, thin-walled. Chlamydospores absent.

Culture characteristics. Colonies on PDA growing in the dark with an average growth rate of 6.2 mm/d at 25 °C. Colony surface white to red, flat or slightly raised at the center; colony margins regular, round. Reverse red with white periphery. Odor absent. Colonies on SNA incubated at 25 °C in the dark were regular, round, growing at 5.4 mm/d. Colony surface pure white, aerial mycelium abundant. Reverse pure white, without diffusible pigments. Colonies on OMA incubated at 25 °C in the dark were regular, round, aerial mycelium abundant, loose to densely floccose, growing at 6.0 mm/d. Reverse red with white periphery. Colonies on CMA incubated at 25 °C in the dark were regular, round, colony surface and reverse red with white periphery, aerial mycelium absent or scant, growing at 7.1 mm/d.

Additional materials examined. China, Fujian Province, Nanping City, Shunchang County, Yangkou Forest Farm, 26°48'36"N, 117°52'48"E, isolated from leaf spots of *Cunninghamia lanceolata*, May 2017, Wen-Li Cui, isolates: LC14-1, LC14-2, LC14-3.

Notes. The isolates of *F. fujianense* were phylogenetically closely related to *F. citri-sinensis* (ex-type, YZU 191316), *F. cassiae* (ex-holotype, MFLUCC 18-0573), and *F. stilboides* (ex-type, CBS 746.79) (Fig. 2). Between *F. fujianense* isolates and ex-type of *F. citri-sinensis* YZU 191316, there were 13/672 differences in *TEF-1α*, and 8/776 in *RPB2*. Between *F. fujianense* isolates and ex-holotype of *F. cassiae* MFLUCC 18-0573, there were 25/672 differences in *TEF-1α*, and 7/776 in *RPB2*. Between *F. fujianense* isolates and ex-type of *F. stilboides* CBS 746.79, there were 16/672 differences in *TEF-1α*, and 2/776 in *RPB2*. The *RPB1* sequences of *F. stilboides* CBS 746.79, *F. cassiae* MFLUCC 18-0573, and *F. citri-sinensis* YZU 191316 were missing. The PHI analysis showed that there was no significant recombination between *F. fujianense* isolates and its related species (Φw = 0.2461) (Fig. 3A). Morphologically, *F. fujianense* differed from *F. citri-sinensis* in colony characteristics on PDA. The former developed dense mycelia and abundant red pigmentation, while the latter was characterized by sparse and loose aerial mycelia and pale pink pigment (Zhao et al. 2022). *F. fujianense* can be differentiated from *F. cassiae* in having abundant red pigmentation produced in PDA vs. without diffusible pigments in *F. cassiae* (Perera et al. 2020). *F. fujianense* can be distinguished from *F. stilboides* by having different 0-septate conidia (5.6–8.3 × 1.9–2.7 µm vs. 7–14 × 2–2.5 µm) (Booth and Waterston 1964). Thus, *F. fujianense* is recognized as a novel species in *F. lateritium* species complex.

Fusarium guizhouense **Lin Huang, Jiao He & D.W. Li, sp. nov.**

Index Fungorum Number: IF900474

Fig. 7

Etymology. Epithet is after Guizhou Province where the type specimen was collected.

Holotype. China, Guizhou Province, Qiandongnan Miao and Dong Autonomous Prefecture, Cengong County, Kelou Town, 27°22'58"N, 108°22'9"E, isolated

from leaf spots of *Cunninghamia lanceolata*, May 2017, Wen-Li Cui, (holotype: CFCC 57575). Holotype specimen is a living specimen maintained via lyophilization at the China Forestry Culture Collection Center (CFCC). Ex-type (GZ7-20-1) is maintained at the Forest Pathology Laboratory, Nanjing Forestry University.

Host/distribution. From *C. lanceolata* in Kelou Town, Cengong County, Qiandongnan Miao and Dong Autonomous Prefecture, Guizhou Province, China.

Description. Sexual state not observed. Asexual state: Sporulation abundant from sporodochia, rarely from conidiophores formed directly on the substrate mycelium. Conidiophores in the aerial mycelium absent. Sporodochia bright orange colored, formed abundantly on carnation leaves. Conidiophores in sporodochia (13.8–)18.8–25.8(–29.8) µm, (mean ± SD = 22.3 ± 3.5 µm, n = 39), irregularly branched and densely packed, bearing apical whorls of 1–4 phialides; sporodochial phialides subulate to subcylindrical, (8.2–)10.6–14.7(–16.9) × (2.7–)3.1–4.0(–4.8) µm, (mean ± SD = 12.6 ± 2.0 × 3.6 ± 0.5 µm, n = 40), smooth, thin-walled. Sporodochial macroconidia colorless, straight or slightly curved, wider at the middle or apical part, tapering towards the base, with a blunt and often curved apical cell and a foot-like to slightly notched basal cell, 4–5-septate. Four-septate conidia: (30.8–)33.3–40.9(–40.6) × (4.5–)5.3–6.4(–6.9) µm, (mean ± SD = 37.1 ± 3.8 × 5.9 ± 0.5 µm, n = 52), five-septate conidia: (33.4–)38.0–45.4(–51.3) × (5.0–)5.7–6.9(–7.5) µm, (mean ± SD = 41.7 ± 3.7 × 6.3 ± 0.6 µm, n = 60), smooth, thin-walled. Chlamydospores absent.

Culture characteristics. Colonies on PDA growing in the dark with an average growth rate of 16.7 mm/d at 25 °C. Colony color white at first, becoming buff, felty to cottony. Aerial mycelium abundant, loose to densely floccose; margins irregular and fimbriate. Reverse pale buff with white periphery. Odor absent. Colonies on SNA incubated at 25 °C in the dark were irregular, growing at 9.7 mm/d. Colony surface pure white, aerial mycelium scant, forming irregular rings at the periphery of the colony; margins lobate or serrate. Reverse pure white, without diffusible pigments. Colonies on OMA incubated at 25 °C in the dark were irregular, aerial mycelium abundant, loose to densely floccose, growing at 13.1 mm/d. Colony in reverse was white with litter gray pigmentation. Colonies on CMA incubated at 25 °C in the dark were round, colony surface and reverse white, flat, radially striated, membranous to dusty, aerial mycelium scant or absent; colony margins irregular, lobate or serrate, growing at 9.6 mm/d.

Additional materials examined. China, Guizhou province, Qiandongnan Miao and Dong Autonomous Prefecture, Cengong County, Kelou Town, 27°22'58"N, 108°22'9"E, isolated from leaf spots of *Cunninghamia lanceolata*, May 2017, Wen-Li Cui, isolates: GZ7-20-1-1, GZ7-20-1-2, GZ7-20-1-3.

Notes. The isolates of *F. guizhouense* were phylogenetically close to *F. sambucinum* (ex-holotype, CBS 146.95), *F. poae* (ex-type, NRRL 26941), and *F. venenatum* (ex-type, CBS 458.93) (Fig. 5). Between *F. guizhouense* isolates and ex-holotype of *F. sambucinum* CBS 146.95, there were 34/577 differences in *TEF-1α*, 8/897 in *RPB2*. The *RPB1* sequence of *F. sambucinum* CBS 146.95 was missing. Between *F. guizhouense* isolates and ex-type of *F. poae* NRRL 26941, there were 24/897 differences in *RPB2*, 26/641 in *RPB1*. The *TEF-1α* sequence of *F. poae* NRRL 26941 was missing. Between *F. guizhouense* isolates and ex-type of *F. venenatum* CBS 458.93, there were 20/577 differences in *TEF-1α*, 8/897 in *RPB2*. The *RPB1* sequence of *F. venenatum* CBS 458.93 was missing. The PHI analysis showed that there was no significant recombination between *F. guizhouense* isolates and

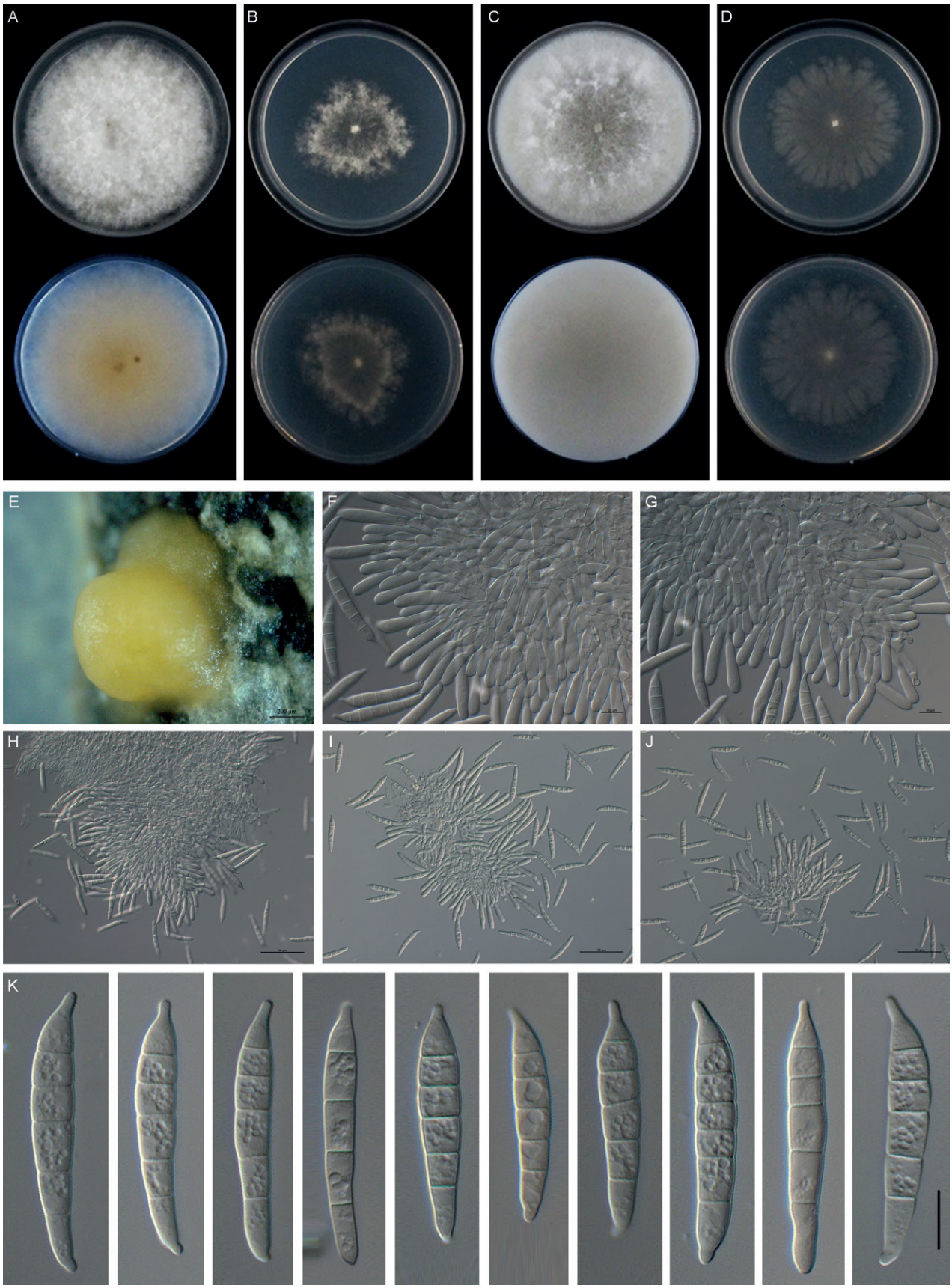

Figure 7. *Fusarium guizhouense* (GZ7-20-1) **A–D** colonies on PDA, SNA, OMA, and CMA, respectively, after 5 days at 24 °C in the dark **E** sporodochia formed on the surface of carnation leaves **F–J** sporodochial conidiophores, phialides, and macroconidia **K** macroconidia (4–6-septate). Scale bars: 200 μm (**E**); 10 μm (**F, G, K**); 50 μm (**H–J**).

its related species (Φ_w = 0.7313) (Fig. 3C). Morphologically, Sporodochial phialides of the *F. guizhouense* isolates (10.6–14.7 × 3.1–4.0 µm) were smaller than those of *F. sambucinum* NRRL 22203 (ex-lectotype) (14.0–18.0 × 3.8–4.5 µm) (Nirenberg 1995). *Fusarium* sp. FSAMSC_11 (NRRL 22192) is closely related to *F. guizhouense*, but it has no morphological data available (Laraba et al. 2021). Further study on this isolate (NRRL 22192) is necessary to determine its taxonomic placement. In conclusion, the phylogenetic and morphological evidence support this fungus being a new species within the *F. sambucinum* species complex.

Fusarium hunanense **Lin Huang, Jiao He & D.W. Li, sp. nov.**

Index Fungorum Number: IF900475

Fig. 8

Etymology. Epithet is named after Hunan Province where the type specimen was collected.

Holotype. China, Hunan Province, Yiyang City, Heshan District, Henglongqiao Town, 28°27'24"N, 112°29'7"E, isolated from leaf spots of *Cunninghamia lanceolata*, May 2017, Wen-Li Cui, (holotype: CFCC 57574). Holotype specimen is a living specimen maintained via lyophilization at the China Forestry Culture Collection Center (CFCC). Ex-type (HN33-8-2) is maintained at the Forest Pathology Laboratory, Nanjing Forestry University.

Host/distribution. From *C. lanceolata* in Henglongqiao Town, Heshan District, Yiyang City, Hunan Province, China.

Description. Sexual state not observed. Asexual state: sporulation abundant from erect conidiophores formed on the agar surface or aggregated in sporodochia. Conidiophores in the aerial mycelium, mostly unbranched, rarely basally dichotomously branched, forming monophialides on the apices; phialides slender, subulate to subcylindrical, monophialidic, smooth, thin-walled, (29.6–)31.6–54.6(–74.1) × (2.0–)2.2–2.8(–3.0) µm, (mean ± SD = 43.1± 11.5 × 2.5 ± 0.3 µm, n = 17), with slight periclinal thickening at the tip and a short flared apical collarette. Sporodochia cream colored, produced on the surface of carnation leaves and PDA medium. Conidiophores in sporodochia (26.0–)29.3–39.1(–46.8) µm, (mean ± SD = 34.1 ± 5.1 µm, n = 39), irregularly branched, short stipitate, occasionally in whorls bearing terminal 2–4 monophialides; sporodochial phialides subulate to subcylindrical, smooth, thin-walled, (11.4–)15.5–22.1(–28.6) × (3.3–)4.0–5.2(–6.0) µm, (mean ± SD = 18.8 ± 3.3 × 4.6 ± 0.6 µm, n = 51), with periclinal thickening and a small, flared collarette. Sporodochial macroconidia cylindrical to falcate, gently curved, typically with a blunt and almost rounded apical cell and a barely notched foot cell, 3–6-septate, hyaline, smooth, thin-walled. Three-septate conidia: (22.1–)22.6–39.4(–54.7) × (5.0–)5.5–6.7(–7.4) µm, (mean ± SD = 31.0 ± 8.4 × 6.1 ± 0.6 µm, n = 11); four-septate conidia: (50.3–)54.4–68.2(–69.6) × (6.9–)6.9–7.7(–8.0) µm, (mean ± SD = 61.3 ± 6.9 × 7.3 ± 0.4 µm, n = 10); five-septate conidia: (51.8–)60.6–73.0(–78.2) × (6.4–)6.1–7.1(–8.5) µm, (mean ± SD = 66.8 ± 6.2 × 6.6 ± 0.5 µm, n = 31); six-septate conidia: (69.8–)70.7–77.7(–79.6) × (7.1–)7.5–8.3(–8.3) µm, (mean ± SD = 74.2 ± 3.5 µm × 7.9 ± 0.4 µm, n = 10). Chlamydospores developed in large numbers in hyphae and also in mature macroconidia. The chlamydospores were 0–1-septate, globose to ellipsoidal, constricted at the septum, intercalary or terminal

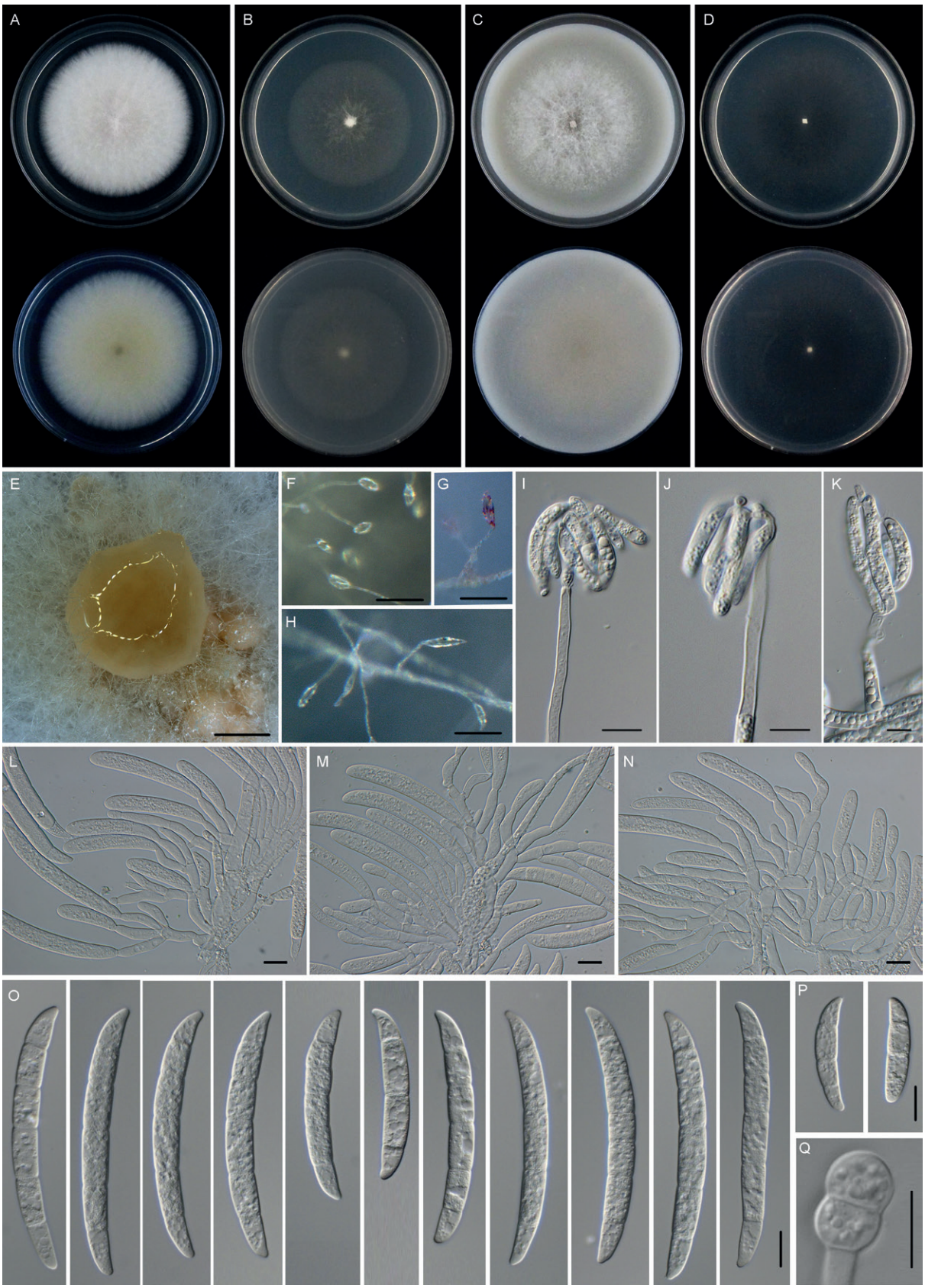

Figure 8. *Fusarium hunanense* (HN33-8-2) **A–D** colonies on PDA, SNA, OMA, and CMA, respectively, after 5 days at 24 °C in the dark **E** sporodochia formed on PDA **F–K** aerial conidiophores, phialides, and conidia **L–N** sporodochial conidiophores, phialides, and conidia **O, P** macroconidia (3–6-septate) **Q** chlamydospore. Scale bars: 1,000 µm (**E**); 50 µm (**F–H**); 10 µm (**I–Q**).

in chains or solitary with mostly a pale color and smooth, (11.7–)11.7–12.9(–13.5) × (7.7–)7.7–8.5(–8.6) µm, (mean ± SD = 12.3 ± 0.6 × 8.1 ± 0.4 µm, n = 6).

Culture characteristics. Colonies on PDA growing in the dark with an average growth rate of 9.2 mm/d at 25 °C. Colony color white, flat, margins regular and fimbriate. Aerial mycelia abundant. Odor absent. Reverse white to pale luteous. Colonies on SNA incubated at 25 °C in the dark growing at 7.2 mm/d. Colony surface pure white, aerial mycelium scant. Reverse pure white, without diffusible pigments. Colonies on OMA incubated at 25 °C in the dark growing at 10.1 mm/d, color white, flat, velvety to felty with abundant floccose aerial mycelium. Reverse white without diffusible pigments. Colonies on CMA incubated at 25 °C in the dark were round, colony surface and reverse white, flat, aerial mycelium absent, hyphae hyaline, growing at 9.1 mm/d.

Additional materials examined. China, Hunan province, Yiyang City, Heshan District, Henglongqiao Town, 28°27'24"N, 112°29'7"E, isolated from leaf spots of *Cunninghamia lanceolata*, May 2017, Wen-Li Cui, isolates: HN33-8-2-1, HN33-8-2-2, HN33-8-2-3.

Notes. The isolates of *F. hunanense* were phylogenetically close to *F. pseudensiforme* (ex-type, CBS 125729) (Fig. 4). Between *F. hunanense* isolates and ex-type of *F. pseudensiforme* CBS 125729, there were 8/583 differences in *TEF-1α*, 3/800 in *RPB2*, and 9/640 in *RPB1*. The PHI analysis showed that there was no significant recombination among *F. hunanense* isolates and its related species (Φ_w = 1.0) (Fig. 3B). Morphologically, 5-septate sporodochial macroconidia of the *F. hunanense* isolates (60.6–73.0 × 6.1–7.1 µm) were longer than those of *F. pseudensiforme* CBS 125729 (ex-type) (50–63 × 5.2–7.2 µm) (Nalim et al. 2011). In conclusion, the phylogenetic and morphological evidence supported this fungus being a new species within the *F. solani* species complex.

Pathogenicity assays. Pathogenicity was tested on detached *C. lanceolata* leaves *in vitro* following Koch's postulates for *F. hunanense* (HN33-8-2), *F. concentricum* (SJ1-10), *F. guizhouense* (GZ7-20-1), *F. fujikuroi* (HN43-17-1), and *F. fujianense* (LC14). At five days post-inoculation, all the tested isolates caused leaf necrosis, with dark brown lesions. The control remained unchanged (Fig. 9A). Equivalently, shoots of tissue-culture seedlings of *C. lanceolata* were inoculated by *F. hunanense* (HN33-8-2), *F. concentricum* (SJ1-10), *F. guizhouense* (GZ7-20-1), *F. fujikuroi* (HN43-17-1), and *F. fujianense* (LC14) *in vivo*. After ten days post-inoculation, all isolates caused necrotic lesions on shoots of *C. lanceolata*. The control remained healthy (Fig. 9B). Statistically, these isolates showed different levels of virulence. *Fusarium hunanense* (HN33-8-2) was significantly more virulent than those of *F. concentricum* (SJ1-10), *F. guizhouense* (GZ7-20-1), *F. fujikuroi* (HN43-17-1), and *F. fujianense* (LC14), while *F. fujianense* (LC14) was the least virulent (Fig. 9C).

The fungal isolates used for inoculation were re-isolated from the diseased spots on the inoculated leaves and shoots, but no fungus was isolated from the leaves and shoots of the control. Koch's postulates were satisfied, and these isolates HN33-8-2, SJ1-10, GZ7-20-1, HN43-17-1, and LC14 were determined to be the pathogens of leaf blight on *C. lanceolata*.

Discussion

In this study, the pathogens causing leaf blight of *C. lanceolata* in China, focusing especially on Fujian, Guangxi, Guizhou, and Hunan provinces, were determined

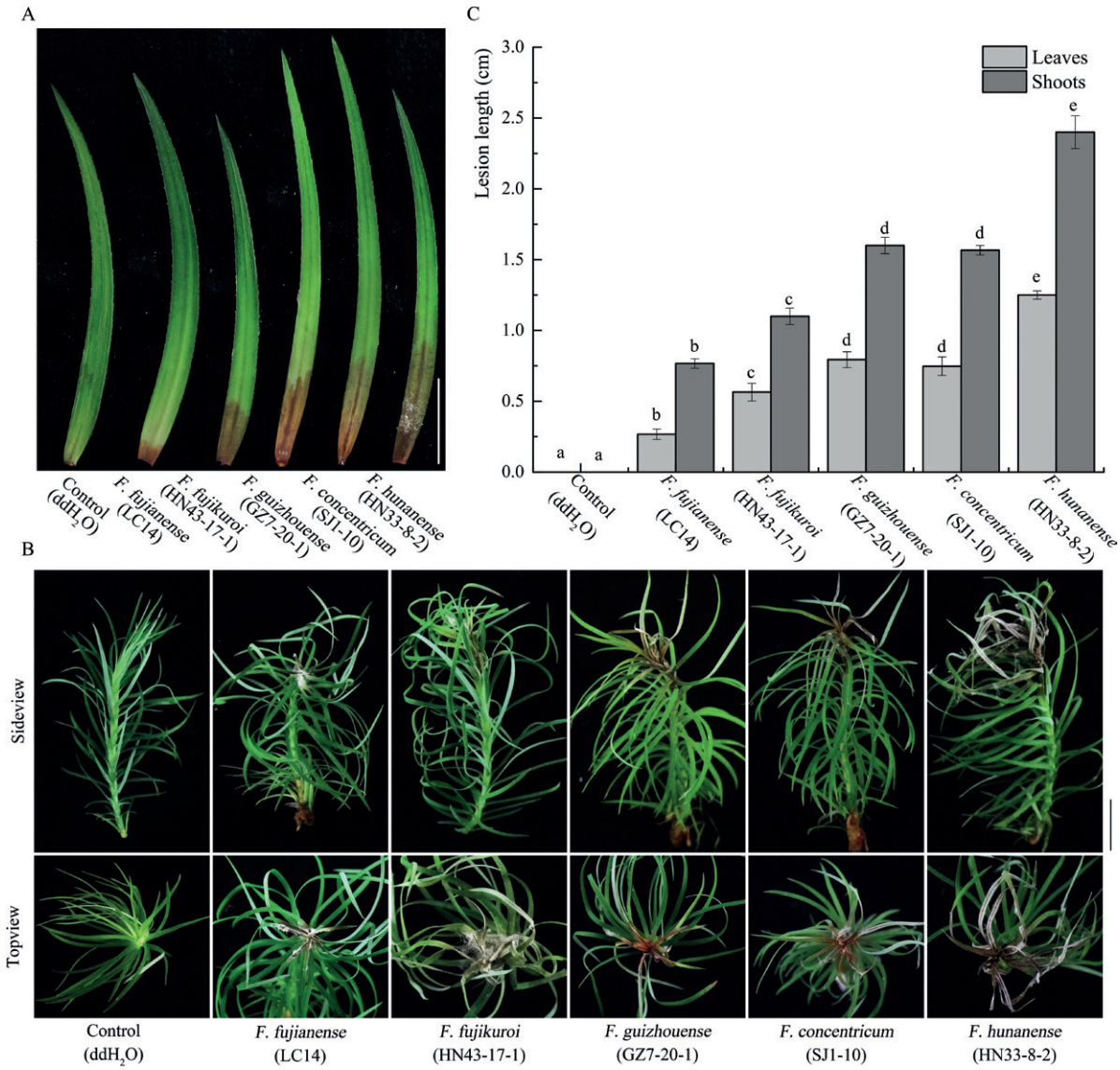

Figure 9. Symptoms on detached *Cunninghamia lanceolata* leaves (**A**) and shoots of tissue-culture seedlings of *C. lanceolata* (**B**) inoculated with isolates: *Fusarium fujianense* (LC14), *F. fujikuroi* (HN43-17-1), *F. guizhouense* (GZ7-20-1), *F. concentricum* (SJ1-10), and *F. hunanense* (HN33-8-2). Scale bar: 10 mm. C, Lesion length on detached *C. lanceolata* leaves inoculated with *F. fujianense* (LC14), *F. fujikuroi* (HN43-17-1), *F. guizhouense* (GZ7-20-1), *F. concentricum* (SJ1-10), and *F. hunanense* (HN33-8-2). Error bars represent standard deviation, and different letters indicate significant difference based on LSD's range test at $P < 0.05$ (n = 8).

by the inoculation tests using the shoots of tissue-culture seedlings of *C. lanceolata*. Phylogenetic and morphological analyses were used to evaluate the diversity of *Fusarium* species from the symptomatic *C. lanceolata* leaves. Three of the species newly described here (*F. fujianense*, *F. hunanense*, and *F. guizhouense*) and two known species (*F. fujikuroi* and *F. concentricum*) were associated with leaf blight of *C. lanceolata*. To date, *F. oxysporum* f. *pini* has been reported from *C. lanceolata* in Taiwan, China (Anonymous 1979). *Fusarium oxysporum* and *Fusarium* sp. have been reported to cause *C. lanceolata* seedlings damping off in mainland China (Chen 2002; Tian et al. 2019). However, none of the five species of *Fusarium* were previously reported to be pathogens of this disease. The taxonomic and phylogenetic analyses are the basis of research for various fields of

Fusarium biology. Because often *Fusarium* isolates show morphological variation during their growth in culture, their identification faces certain difficulties and challenges. Microscopically, the most typical feature of the genus *Fusarium s.l.* is its identifiable spindle- or canoe-shaped macroconidia (hyaline, multicellular, in clusters, macroconidia with or without foot cells at the base). If microconidia are present, the shape, number of cells, and mode of conidiogenesis (chains or false heads) are important in identification (Leslie and Summerell 2006).

Phylogenetic analyses based on DNA sequence diversity plays a crucial role, and many molecular markers, such as ITS, *TUB2*, *HIS3*, and *CAL* etc. have been used. However, *RPB2* and *TEF-1α* sequences appear to be the most useful in taxonomic studies of fungi, especially for the members of the genus *Fusarium* (O'Donnell 2000; O'Donnell et al. 2013; Crous et al. 2021). In the previous results of this study, it was found that, compared to *TEF-1α* and *RPB2* gene sequences, the ITS possesses relatively little phylogenetic signal, and the *TUB2* sequence is too short, thus the two loci have been eliminated. In the present study, the phylogeny inferred from concatenate multi-locus sequences (*TEF-1α*, *RPB2*, and *RPB1*) as suggested from previous studies (Sandoval-Denis et al. 2018) grouped isolates from *C. lanceolata* into five species belonging to four *Fusarium* species complexes with high supports. It should be noted here that, *TEF-1α*, *RPB2* and *RPB1* genes used to distinguish these species have rich information, but relatively few *RPB1* sequences are available in the databases, so there were some limitations using *RPB1*.

At present, the taxonomic studies on *Fusarium* are very divisive, especially segregating the *Fusarium solani* species complex as *Neocosmospora* (Lombard et al. 2015; de Hoog et al. 2023). The disagreement has become wider in recent years. Both sides have their support. In addition to the previous publications, the studies published in 2023 reflect such a dilemma. Chen et al. (2023) recognized nine genera of fusarioid and considered these nine genera are well-supported in their present phylogenomic study and different from *Fusarium*, while Zeng and Zhuang (2023) recognized 14 genera. At the same time, some mycologists, plant pathologists, and medical mycologists supported the broad concept of *Fusarium* and preferred the species complexes of *Fusarium*. *Fusarium bilaiae* Gagkaeva & al., a new cryptic species from sunflower, has been described in the *Fusarium fujikuroi* species complex using the tef, tub, and rpb2 sequences (Gagkaeva et al. 2023). In a Brazilian study on *Fusarium* from melons, Silva et al. (2023) favored *Fusarium solani* species complex (FSSC) and reported that among the 31 isolates, 29 isolates were *Fusarium falciforme* (Carrión) Summerb. & Schroers, (=*Neocosmospora falciformis* (Carrión) L. Lombard & Crous) and two isolates were *F. suttonianum* (Sand.-Den. & Crous) O'Donnell, Geiser & T. Aoki (≡*Neocosmospora suttoniana* Sand.-Den. & Crous) using sequences of *EF-1α* and *RPB2*. The position paper by de Hoog et al. (2023) to the medical community showed how complicated the disagreement has become at present. de Hoog et al. (2023) indicated that the phylogenetic relationship between *Fusarium* and *Neocosmospora* may justify their segregation, and it seems necessary to maintain the fusarium-like genera proposed by Crous et al. (2021). However, de Hoog et al. (2023) also opined that the segregation of *Neocosmospora* was not obligatory for the medical fields to be adopted immediately and recommended waiting until taxonomists settle their disagreement (de Hoog et al. 2023). Thus, de Hoog et al. (2023) recommended using the names under *Fusarium* species complexes, not the names under the segregated genera. This is the opinion with which we agree.

Species delineation needs polyphasic support. In addition to phylogenetic analyses and morphological studies, genealogical concordance analysis enables to determine sexual recombination and provides an operational criterion to verify the species borderline (de Hoog et al. 2023). This method was used in our present studies and no significant genetic recombination was in the new species that we described.

Pathogenicity tests showed that all five species were able to infect host plants. However, these species displayed differences in virulence on *C. lanceolata*. It is well known that *F. fujikuroi* is the causal agent of the rice disease bakanae in the major rice-growing regions in the world (Leslie and Summerell 2006). Besides rice, *F. fujikuroi* has been reported as saprobe or endophyte of vanilla (Pinaria et al. 2010) and isolated from human skin (O'Donnell et al. 2010). However, the predominant presence of *F. fujikuroi* from leaves of *C. lanceolata* has not been reported. This result could also be explained by the crop planting history of the sample site. We speculated that the fields have been previously planted with rice, which are highly susceptible to *F. fujikuroi* among other *Fusarium* species. *Fusarium concentricum* was described as a new species by Nirenberg and O'Donnell (1998), which was predominantly isolated from *Musa* × *paradisiaca* (banana) in Central America and *Nilaparvata lugens* (Asian brown leaf hopper) in South Korea. *Nilaparvata lugens* is a serious pest on rice in Asia (Wu et al. 2018). It is possible that this insect serves as a vector for this pathogen's dispersal. Very little is known about the pathogenicity and biology of *F. concentricum* (Leslie and Summerell 2006). However, *F. fujikuroi* and *F. concentricum* are reported to cause leaf blight on *C. lanceolata* for the first time.

The present study introduces new insights into the biodiversity of *Fusarium* species associated with *C. lanceolata* in China. A remarkable diversity of *Fusarium* species spanning several species complexes was found from four provinces, China. Furthermore, three new species of *Fusarium* were described, with demonstrated pathogenicity to *C. lanceolata*. However, considering the limited geographic areas studied, it is likely that additional *Fusarium* species would also be isolated if more areas were studied. Meanwhile, this also shows that despite the widespread distribution of *C. lanceolata* in China, and previous knowledge about its associated microbes, the fungal species-richness in *C. lanceolata* remains underestimated. Therefore, more studies are necessary on these new taxa in order to elucidate their host range, specificity, and global distribution, as well as their potential impact on the *C. lanceolata* industry.

Additional information

Conflict of interest

The authors have declared that no competing interests exist.

Ethical statement

No ethical statement was reported.

Funding

This research was supported by the Nature Science Foundation of China (31870631), the National Key R & D Program of China (2017YFD0600102), Qing Lan Project, and Priority Academic Program Development of Jiangsu Higher Education Institutions (PAPD).

Author contributions

LHZ and LH designed research; JH and WLC performed experiments; JH, DWL and LHZ analyzed data; JH wrote the original draft; and DWL and LH reviewed and edited the manuscript. All authors have read and approved the final manuscript.

Author ORCIDs

Jiao He https://orcid.org/0000-0002-4146-2223
De-Wei Li https://orcid.org/0000-0002-2788-7938
Wen-Li Cui https://orcid.org/0009-0005-7515-7672
Li-Hua Zhu https://orcid.org/0000-0003-2740-4980
Lin Huang https://orcid.org/0000-0001-7536-0914

Data availability

All of the data that support the findings of this study are available in the main text or Supplementary Information.

References

Anonymous (1979) List of Plant Diseases in Taiwan. Pl. Protect. Soc., Republ. of China, 404 pp.

Aoki T, O'Donnell K, Geiser DM (2014) Systematics of key phytopathogenic *Fusarium* species: Current status and future challenges. Journal of General Plant Pathology 80(3): 189–201. https://doi.org/10.1007/s10327-014-0509-3

Aoki T, Geiser DM, Kasson MT, O'Donnell K (2020) Nomenclatural novelties. Index Fungorum: Published Numbers 440(3): 1–5.

Aoki T, Geiser DM, O'Donnell K (2021a) Nomenclatural novelties. Index Fungorum: Published Numbers 496: 1–2.

Aoki T, Geiser DM, O'Donnell K (2021b) Nomenclatural novelties. Index Fungorum: Published Numbers 486: 1.

Boonpasart S, Kasetsuwan N, Puangsricharern V, Pariyakanok L, Jittpoonkusol T (2002) Infectious keratitis at King Chulalongkorn Memorial Hospital: a 12-year retrospective study of 391 cases. Journal of the Medical Association of Thailand = Chotmaihet thangphaet 85 Suppl 1: S217–230.

Booth C, Waterston J (1964) *Fusarium stilboides*. [Descriptions of Fungi and Bacteria]. CABI International, Sheet, 30 pp.

Burgess LW, Liddell CM, Summerell BA (1988) Laboratory manual for fusarium research: incorporating a key and descriptions of common species found in Australasia (2nd ed.). University of Sydney S, Australia.

Chen MM (2002) Forest Fungi Phytogeography: Forest Fungi Phytogeography of China, North America, and Siberia and International Quarantine of Tree Pathogens. Pacific Mushroom Research and Education Center, Sacramento, California, 469 pp.

Chen YP, Su PW, Hyde K, Maharachchikumbura S (2023) Phylogenomics and diversification of Sordariomycetes. Mycosphere 14(1): 414–451. https://doi.org/10.5943/mycosphere/14/1/5

Chung PC, Wu HY, Wang YW, Ariyawansa HA, Hu HP, Hung TH, Tzean SS, Chung CL (2020) Diversity and pathogenicity of *Colletotrichum* species causing strawberry anthracnose in Taiwan and description of a new species, *Colletotrichum miaoliense* sp. nov. Scientific Reports 10(1): e14664. https://doi.org/10.1038/s41598-020-70878-2

Coleman JJ (2016) The *Fusarium solani* species complex: Ubiquitous pathogens of agricultural importance. Molecular Plant Pathology 17(2): 146–158. https://doi.org/10.1111/mpp.12289

Crous PW, Lombard L, Sandoval-Denis M, Seifert KA, Schroers HJ, Chaverri P, Gené J, Guarro J, Hirooka Y, Bensch K, Kema GHJ, Lamprecht SC, Cai L, Rossman AY, Stadler M, Summerbell RC, Taylor JW, Ploch S, Visagie CM, Yilmaz N, Frisvad JC, Abdel-Azeem AM, Abdollahzadeh J, Abdolrasouli A, Akulov A, Alberts JF, Araújo JPM, Ariyawansa HA, Bakhshi M, Bendiksby M, Ben Hadj Amor A, Bezerra JDP, Boekhout T, Câmara MPS, Carbia M, Cardinali G, Castañeda-Ruiz RF, Celis A, Chaturvedi V, Collemare J, Croll D, Damm U, Decock CA, de Vries RP, Ezekiel CN, Fan XL, Fernández NB, Gaya E, González CD, Gramaje D, Groenewald JZ, Grube M, Guevara-Suarez M, Gupta VK, Guarnaccia V, Haddaji A, Hagen F, Haelewaters D, Hansen K, Hashimoto A, Hernández-Restrepo M, Houbraken J, Hubka V, Hyde KD, Iturriaga T, Jeewon R, Johnston PR, Jurjević Ž, Karalti I, Korsten L, Kuramae EE, Kušan I, Labuda R, Lawrence DP, Lee HB, Lechat C, Li HY, Litovka YA, Maharachchikumbura SSN, Marin-Felix Y, Matio Kemkuignou B, Matočec N, McTaggart AR, Mlčoch P, Mugnai L, Nakashima C, Nilsson RH, Noumeur SR, Pavlov IN, Peralta MP, Phillips AJL, Pitt JI, Polizzi G, Quaedvlieg W, Rajeshkumar KC, Restrepo S, Rhaiem A, Robert J, Robert V, Rodrigues AM, Salgado-Salazar C, Samson RA, Santos ACS, Shivas RG, Souza-Motta CM, Sun GY, Swart WJ, Szoke S, Tan YP, Taylor JE, Taylor PWJ, Tiago PV, Váczy KZ, van de Wiele N, van der Merwe NA, Verkley GJM, Vieira WAS, Vizzini A, Weir BS, Wijayawardene NN, Xia JW, Yáñez-Morales MJ, Yurkov A, Zamora JC, Zare R, Zhang CL, Thines M (2021) Fusarium: More than a node or a foot-shaped basal cell. Studies in Mycology 98(4): e100116. https://doi.org/10.1016/j.simyco.2021.100116

Cui WL, Bian JY, Li DW, Wang JW, Huang L (2020a) First report of leaf blight on Chinese fir (*Cunninghamia lanceolata*) caused by *Bipolaris setariae* in China. Plant Disease 104(9): 2523–2523. https://doi.org/10.1094/PDIS-12-19-2685-PDN

Cui WL, Lu XQ, Bian JY, Qi XL, Li DW, Huang L (2020b) *Curvularia spicifera* and *Curvularia muehlenbeckiae* causing leaf blight on *Cunninghamia lanceolata*. Plant Pathology 69(6): 1139–1147. https://doi.org/10.1111/ppa.13198

Dai XK, Zhang ML, Liu T, Chen XY, Zhu TH (2023) Brown leaf spot of *Cunninghamia lanceolata* caused by *Colletotrichum kahawae* in Sichuan province, China. Plant Disease 107(8): e2548. https://doi.org/10.1094/PDIS-12-22-2794-PDN

Damm U, Mostert L, Crous PW, Fourie PH (2008) Novel *Phaeoacremonium* species associated with necrotic wood of *Prunus* trees. Persoonia 20(1): 87–102. https://doi.org/10.3767/003158508X324227

de Hoog S, Walsh TJ, Ahmed SA, Alastruey-Izquierdo A, Alexander BD, Arendrup MC, Babady E, Bai FY, Balada-Llasat J-M, Borman A, Chowdhary A, Clark A, Colgrove R, Cornely O, Dingle T, Dufresne P, Fuller J, Gangneux J-P, Gibas C, Zhang S (2023) A conceptual framework for nomenclatural stability and validity of medically important fungi: A proposed global consensus guideline for fungal name changes supported by ABP, ASM, CLSI, ECMM, ESCMID-EFISG, EUCAST-AFST, FDLC, IDSA, ISHAM, MMSA, and MSGERC. Journal of Clinical Microbiology 61(11): e00873–e00823. https://doi.org/10.1128/jcm.00873-23

Dean R, Van Kan JAL, Pretorius ZA, Hammond-Kosack K, Di Pietro A, Spanu PD, Rudd JJ, Dickman M, Kahmann R, Ellis J, Foster GD (2012) The Top 10 fungal pathogens in molecular plant pathology. Molecular Plant Pathology 13(4): 414–430. https://doi.org/10.1111/j.1364-3703.2011.00783.x

Gagkaeva T, Orina A, Gomzhina M, Gavrilova O (2023) *Fusarium bilaiae*, a new cryptic species in the *Fusarium fujikuroi* complex associated with sunflower. Mycologia 115(6): 1–15. https://doi.org/10.1080/00275514.2023.2259277

Gams W, Nirenberg HI, Seifert KA, Brayford D, Thrane U (1997) Proposal to conserve the name *Fusarium sambucinum* (Hyphomycetes). Taxon 46(1): 111–113. https://doi.org/10.2307/1224298

Geiser DM, Aoki T, Bacon CW, Baker SE, Bhattacharyya MK, Brandt ME, Brown DW, Burgess LW, Chulze S, Coleman JJ, Correll JC, Covert SF, Crous PW, Cuomo CA, De Hoog GS, Di Pietro A, Elmer WH, Epstein L, Frandsen RJ, Freeman S, Gagkaeva T, Glenn AE, Gordon TR, Gregory NF, Hammond-Kosack KE, Hanson LE, Jímenez-Gasco Mdel M, Kang S, Kistler HC, Kuldau GA, Leslie JF, Logrieco A, Lu G, Lysøe E, Ma LJ, McCormick SP, Migheli Q, Moretti A, Munaut F, O'Donnell K, Pfenning L, Ploetz RC, Proctor RH, Rehner SA, Robert VA, Rooney AP, Bin Salleh B, Scandiani MM, Scauflaire J, Short DP, Steenkamp E, Suga H, Summerell BA, Sutton DA, Thrane U, Trail F, Van Diepeningen A, Vanetten HD, Viljoen A, Waalwijk C, Ward TJ, Wingfield MJ, Xu JR, Yang XB, Yli-Mattila T, Zhang N (2013) One fungus, one name: Defining the genus *Fusarium* in a scientifically robust way that preserves longstanding use. Phytopathology 103(5): 400–408. https://doi.org/10.1094/PHYTO-07-12-0150-LE

Geiser DM, Al-Hatmi AMS, Aoki T, Arie T, Balmas V, Barnes I, Bergstrom GC, Bhattacharyya MK, Blomquist CL, Bowden RL, Brankovics B, Brown DW, Burgess LW, Bushley K, Busman M, Cano-Lira JF, Carrillo JD, Chang HX, Chen CY, Chen W, Chilvers M, Chulze S, Coleman JJ, Cuomo CA, de Beer ZW, de Hoog GS, Del Castillo-Múnera J, Del Ponte EM, Diéguez-Uribeondo J, Di Pietro A, Edel-Hermann V, Elmer WH, Epstein L, Eskalen A, Esposto MC, Everts KL, Fernández-Pavía SP, da Silva GF, Foroud NA, Fourie G, Frandsen RJN, Freeman S, Freitag M, Frenkel O, Fuller KK, Gagkaeva T, Gardiner DM, Glenn AE, Gold SE, Gordon TR, Gregory NF, Gryzenhout M, Guarro J, Gugino BK, Gutierrez S, Hammond-Kosack KE, Harris LJ, Homa M, Hong CF, Hornok L, Huang JW, Ilkit M, Jacobs A, Jacobs K, Jiang C, Jiménez-Gasco MDM, Kang S, Kasson MT, Kazan K, Kennell JC, Kim HS, Kistler HC, Kuldau GA, Kulik T, Kurzai O, Laraba I, Laurence MH, Lee T, Lee YW, Lee YH, Leslie JF, Liew ECY, Lofton LW, Logrieco AF, López-Berges MS, Luque AG, Lysøe E, Ma LJ, Marra RE, Martin FN, May SR, McCormick SP, McGee C, Meis JF, Migheli Q, Mohamed Nor NMI, Monod M, Moretti A, Mostert D, Mulè G, Munaut F, Munkvold GP, Nicholson P, Nucci M, O'Donnell K, Pasquali M, Pfenning LH, Prigitano A, Proctor RH, Ranque S, Rehner SA, Rep M, Rodríguez-Alvarado G, Rose LJ, Roth MG, Ruiz-Roldán C, Saleh AA, Salleh B, Sang H, Scandiani MM, Scauflaire J, Schmale DG III, Short DPG, Šišić A, Smith JA, Smyth CW, Son H, Spahr E, Stajich JE, Steenkamp E, Steinberg C, Subramaniam R, Suga H, Summerell BA, Susca A, Swett CL, Toomajian C, Torres-Cruz TJ, Tortorano AM, Urban M, Vaillancourt LJ, Vallad GE, van der Lee TAJ, Vanderpool D, van Diepeningen AD, Vaughan MM, Venter E, Vermeulen M, Verweij PE, Viljoen A, Waalwijk C, Wallace EC, Walther G, Wang J, Ward TJ, Wickes BL, Wiederhold NP, Wingfield MJ, Wood AKM, Xu JR, Yang XB, Yli-Mattila T, Yun SH, Zakaria L, Zhang H, Zhang N, Zhang SX, Zhang X (2021) Phylogenomic analysis of a 55.1-kb 19-gene dataset resolves a monophyletic *Fusarium* that includes the *Fusarium solani* species complex. Phytopathology 111(7): 1064–1079. https://doi.org/10.1094/PHYTO-08-20-0330-LE

Gerlach W, Nirenberg HI (1982) The genus *Fusarium*: A pictorial atlas. Mitteilungen aus der Biologischen Bundesanstalt fuer Land und Forstwirtschaft. Berlin Dahlem 209: 1–406. https://doi.org/10.2307/3792677

Goswami RS, Kistler HC (2005) Pathogenicity and in planta mycotoxin accumulation among members of the *Fusarium graminearum* species complex on wheat and rice. Phytopathology 95(12): 1397–1404. https://doi.org/10.1094/PHYTO-95-1397

Gräfenhan T, Johnston PR, Vaughan MM, McCormick SP, Proctor RH, Busman M, Ward TJ, O'Donnell K (2016) *Fusarium praegraminearum* sp. nov., a novel nivalenol

mycotoxin-producing pathogen from New Zealand can induce head blight on wheat. Mycologia 108(6): 1229–1239.

He J, Li DW, Zhang Y, Ju YW, Huang L (2021) *Fusarium rosicola* sp. nov. causing vascular wilt on *Rosa chinensis*. Plant Pathology 70(9): 2062–2073. https://doi.org/10.1111/ppa.13452

He J, Li DW, Zhu YN, Si YZ, Huang JH, Zhu LH, Ye JR, Huang L (2022) Diversity and pathogenicity of *Colletotrichum* species causing anthracnose on *Cunninghamia lanceolata*. Plant Pathology 71(8): 1757–1773. https://doi.org/10.1111/ppa.13611

Huang L, Li QC, Zhang Y, Li DW, Ye JR (2016) *Colletotrichum gloeosporioides* sensu stricto is a pathogen of leaf anthracnose on evergreen spindle tree (*Euonymus japonicus*). Plant Disease 100(4): 672–678. https://doi.org/10.1094/PDIS-07-15-0740-RE

Huang L, Zhu YN, Yang JY, Li DW, Li Y, Bian LM, Ye JR (2018) Shoot blight on Chinese fir (*Cunninghamia lanceolata*) is caused by *Bipolaris oryzae*. Plant Disease 102(3): 500–506. https://doi.org/10.1094/PDIS-07-17-1032-RE

Huson DH (1998) SplitsTree: Analyzing and visualizing evolutionary data. Bioinformatics 14(1): 68–73. https://doi.org/10.1093/bioinformatics/14.1.68

Huson DH, Bryant D (2006) Application of phylogenetic networks in evolutionary studies. Molecular Biology and Evolution 23(2): 254–267. https://doi.org/10.1093/molbev/msj030

Ibrahim NF, Mohd MH, Mohamed Nor NMI, Zakaria L (2016) *Fusarium fujikuroi* causing fusariosis of pineapple in peninsular Malaysia. Australasian Plant Disease Notes, Australasian Plant Pathology Society 11(1): 1–21. https://doi.org/10.1007/s13314-016-0206-5

Kalyaanamoorthy S, Minh BQ, Wong TKF, von Haeseler A, Jermiin LS (2017) ModelFinder: Fast model selection for accurate phylogenetic estimates. Nature Methods 14(6): 587–589. https://doi.org/10.1038/nmeth.4285

Katoh K, Standley D (2013) MAFFT multiple sequence alignment software version improvements in performance and usability. Molecular Biology and Evolution 30(4): 772–780. https://doi.org/10.1093/molbev/mst010

Kelly A, Proctor RH, Belzile F, Chulze SN, Clear RM, Cowger C, Elmer W, Lee T, Obanor F, Waalwijk C, Ward TJ (2016) The geographic distribution and complex evolutionary history of the NX-2 trichothecene chemotype from *Fusarium graminearum*. Fungal Genetics and Biology 95: 39–48. https://doi.org/10.1016/j.fgb.2016.08.003

Kobayashi T, Zhao JZ (1987) Two fungi associated with needle blight of *Cunninghamia lanceolata*. Nippon Kingakkai Kaiho 28(3): 289–294.

Kumar S, Glen S, Michael L, Christina K, Koichiro T (2018) MEGA X: Molecular evolutionary genetics analysis across computing platforms. Molecular Biology and Evolution 35(6): 1547–1549. https://doi.org/10.1093/molbev/msy096

Lan X, Dong LJ, Huang KY, Chen DX, Li DW, Mo LY (2015) Main species and prevention research on diseases and pests of *Cunninghamia lanceolata*. Guangxi Forestry Science 44: 162–167. https://doi.org/10.19692/j.cnki.gfs.2015.02.014

Laraba I, McCormick SP, Vaughan MM, Geiser DM, O'Donnell K (2021) Phylogenetic diversity, trichothecene potential, and pathogenicity within *Fusarium sambucinum* species complex. PLOS ONE 16(1): e0245037. https://doi.org/10.1371/journal.pone.0245037

Leslie JF, Summerell BA (2006) The *Fusarium* Laboratory Manual. Blackwell Publishing Professional, USA. https://doi.org/10.1002/9780470278376

Li MF, He J, Ding L, Kang J, Zhang Q, Zheng Q (2007) Single spore strains without producing fruit body isolated from *Cordyceps militeris* and their RAPD analysis. Xi Nan Nong Ye Xue Bao 20: 547–550. https://doi.org/10.16213/j.cnki.scjas.2007.03.050

Li YM, Wang YJ, Jiang GY (2020) Application of origin software in data extraction and analysis in physical chemistry experiments: taking the combustion heat measurement of naphthalene as an example. Education Teaching Forum 50: 375–377.

Li X, He SQ, Gao Y, Xing SJ, Ren H, Yang H, Gao YT, Wang JY, Li NP, Duan JF, Yang J, Huang Q (2022) *Ceratocystis* and related genera causing wilt of *Cunninghamia lanceolata* Yunnan, China. Forest Pathology 52(1): e12744. https://doi.org/10.1111/efp.12744

Liao YCZ, Sun JW, Li DW, Nong ML, Zhu LH (2023) First report of top blight of *Cunninghamia lanceolata* caused by *Diaporthe unshiuensis* and *Diaporthe hongkongensis* in China. Plant Disease 107(3): e962. https://doi.org/10.1094/PDIS-06-22-1467-PDN

Link JHF (1809) Observationes in ordines plantarum naturales. Dissertatio Ima. Gesellschaft Naturforschender Freunde zu Berlin. Magazin 3(1): 3–42.

Liu YJ, Whelen S, Hall BD (1999) Phylogenetic relationships among ascomycetes: Evidence from an RNA polymerse II subunit. Molecular Biology and Evolution 16(12): 1799–1808. https://doi.org/10.1093/oxfordjournals.molbev.a026092

Liu F, Mbenoun M, Barnes I, Roux J, Wingfield MJ, Li G, Li J, Chen S (2015) New *Ceratocystis* species from *Eucalyptus* and *Cunninghamia* in South China. Antonie van Leeuwenhoek 107(6): 1451–1473. https://doi.org/10.1007/s10482-015-0441-3

Lombard L, van der Merwe NA, Groenewald JZ, Crous PW (2015) Generic concepts in Nectriaceae. Studies in Mycology 80(1): 189–245. https://doi.org/10.1016/j.simyco.2014.12.002

Nalim FA, Samuels GJ, Wijesundera RL, Geiser DM (2011) New species from the *Fusarium solani* species complex derived from perithecia and soil in the old world tropics. Mycologia 103(6): 1302–1330. https://doi.org/10.3852/10-307

Nelson PE, Toussoun TA, Marasas WFO (1983) *Fusarium* species: an illustrated manual for identification. Universtity Park, Penn., 193 pp.

Nguyen LT, Schmidt HA, von Haeseler A, Minh BQ (2015) IQ-TREE: A fast and effective stochastic algorithm for estimating maximum-likelihood phylogenies. Molecular Biology and Evolution 32(1): 268–274. https://doi.org/10.1093/molbev/msu300

Nirenberg HI (1995) Morphological differentiation of *Fusarium sambucinum* Fuckel sensu stricto, *F. torulosum* (Berk. & Curt.) Nirenberg comb. nov. and *F. venenatum* Nirenberg sp. nov. Mycopathologia 129(3): 131–141. https://doi.org/10.1007/BF01103337

Nirenberg HI, O'Donnell K (1998) New *Fusarium* species and combinations within the *Gibberella fujikuroi* species complex. Mycologia 90(3): 434–458. https://doi.org/10.1080/00275514.1998.12026929

O'Donnell K (2000) Molecular phylogeny of the *Nectria haematococca-Fusarium solani* species complex. Mycologia 92(5): 919–938. https://doi.org/10.1080/00275514.2000.12061237

O'Donnell K, Kistler HC, Cigelnik E, Ploetz RC (1998) Multiple evolutionary origins of the fungus causing Panama disease of banana: Concordant evidence from nuclear and mitochondrial gene genealogies. Proceedings of the National Academy of Sciences of the United States of America 95(5): 2044–2049. https://doi.org/10.1073/pnas.95.5.2044

O'Donnell K, Nirenberg HI, Aoki T, Cigelnik E (2000) A multigene phylogeny of the *Gibberella fujikuroi* species complex: Detection of additional phylogenetically distinct species. Mycoscience 41(1): 61–78. https://doi.org/10.1007/BF02464387

O'Donnell K, Sutton DA, Rinaldi MG, Sarver BA, Balajee SA, Schroers HJ, Summerbell RC, Robert VA, Crous PW, Zhang N, Aoki T, Jung K, Park J, Lee YH, Kang S, Park B, Geiser DM (2010) Internet-accessible DNA sequence database for identifying fusaria from human and animal infections. Journal of Clinical Microbiology 48(10): 3708–3718. https://doi.org/10.1128/JCM.00989-10

O'Donnell K, Humber RA, Geiser DM, Kang S, Park B, Robert VARG, Crous PW, Johnston PR, Aoki T, Rooney AP, Rehner SA (2012) Phylogenetic diversity of insecticolous fusaria inferred from multilocus DNA sequence data and their molecular identification via FUSARIUM-ID and Fusarium MLST. Mycologia 104(2): 427–445. https://doi.org/10.3852/11-179

O'Donnell K, Rooney AP, Proctor RH, Brown DW, McCormick SP, Ward TJ, Frandsen RJ, Lysøe E, Rehner SA, Aoki T, Robert VA, Crous PW, Groenewald JZ, Kang S, Geiser DM (2013) Phylogenetic analyses of RPB1 and RPB2 support a middle cretaceous origin for a clade comprising all agriculturally and medically important fusaria. Fungal Genetics and Biology 52: 20–31. https://doi.org/10.1016/j.fgb.2012.12.004

O'Donnell K, Ward TJ, Robert VARG, Crous PW, Geiser DM, Kang S (2015) DNA sequence-based identification of *Fusarium*: Current status and future directions. Phytoparasitica 43(5): 583–595. https://doi.org/10.1007/s12600-015-0484-z

O'Donnell K, Al-Hatmi AMS, Aoki T, Brankovics B, Cano-Lira JF, Coleman JJ, de Hoog GS, Di Pietro A, Frandsen RJN, Geiser DM, Gibas CFC, Guarro J, Kim HS, Kistler HC, Laraba I, Leslie JF, López-Berges MS, Lysøe E, Meis JF, Monod M, Proctor RH, Rep M, Ruiz-Roldán C, Šišić A, Stajich JE, Steenkamp ET, Summerell BA, van der Lee TAJ, van Diepeningen AD, Verweij PE, Waalwijk C, Ward TJ, Wickes BL, Wiederhold NP, Wingfield MJ, Zhang N, Zhang SX (2020) No to *Neocosmospora*: Phylogenomic and practical reasons for continued inclusion of the *Fusarium solani* species complex in the genus *Fusarium*. MSphere 5(5): e00810–e00820. https://doi.org/10.1128/mSphere.00810-20

O'Donnell K, Whitaker BK, Laraba I, Proctor RH, Brown DW, Broders K, Kim H-S, McCormick SP, Busman M, Aoki T, Torres-Cruz TJ, Geiser DM (2022) DNA sequence-based identification of *Fusarium*: A work in progress. Plant Disease 106(6): 1597–1609. https://doi.org/10.1094/PDIS-09-21-2035-SR

Perera R, Hyde K, Maharachchikumbura S, Jones E, McKenzie E, Stadler M, Lee H, Samarakoon MC, Ekanayaka A, Erio C, Liu JK (2020) Fungi on wild seeds and fruits. Mycosphere 11(1): 2108–2480. https://doi.org/10.5943/mycosphere/11/1/14

Pinaria AG, Liew ECY, Burgess LW (2010) *Fusarium* species associated with vanilla stem rot in Indonesia. Australasian Plant Pathology 39(2): 176–183. https://doi.org/10.1071/AP09079

Qiu J, Lu Y, He D, Lee YW, Ji F, Xu J, Shi J (2020) *Fusarium fujikuroi* species complex associated with rice, maize, and soybean from Jiangsu province, China: Phylogenetic, pathogenic, and toxigenic analysis. Plant Disease 104(8): 2193–2201. https://doi.org/10.1094/PDIS-09-19-1909-RE

Quaedvlieg W, Binder M, Groenewald JZ, Summerell BA, Carnegie AJ, Burgess TI, Crous PW (2014) Introducing the consolidated species concept to resolve species in the Teratosphaeriaceae. Persoonia 33(1): 1–40. https://doi.org/10.3767/003158514X681981

Rabodonirina M, Piens MA, Monier MF, Guého E, Fière D, Mojon M (1994) *Fusarium* infections in immunocompromised patients: Case reports and literature review. European Journal of Clinical Microbiology & Infectious Diseases 13(2): 152–161. https://doi.org/10.1007/BF01982190

Rambaut A (2014) FigTree v 1.4.2. Institute of evolutionary biology, University of Edinburgh. http://tree.bio.ed.ac.uk/software/figtree/

Ronquist F, Teslenko M, van der Mark P, Ayres DL, Darling A, Hohna S, Larget B, Liu L, Suchard MA, Huelsenbeck JP (2012) MrBayes 3.2: Efficient Bayesian phylogenetic inference and model choice across a large model space. Systematic Biology 61(3): 539–542. https://doi.org/10.1093/sysbio/sys029

Rossman AY, Samuels GJ, Rogerson CT, Lowen R (1999) Genera of Bionectriaceae, Hypocreaceae and Nectriaceae (Hypocreales, Ascomycetes). Studies in Mycology 42(42): 1–248.

Sandoval-Denis M, Crous PW (2018) Removing chaos from confusion: Assigning names to common human and animal pathogens in *Neocosmospora*. Persoonia 41(1): 109–129. https://doi.org/10.3767/persoonia.2018.41.06

Sandoval-Denis M, Guarnaccia V, Polizzi G, Crous PW (2018) Symptomatic citrus trees reveal a new pathogenic lineage in *Fusarium* and two new *Neocosmospora* species. Persoonia 40(1): 1–25. https://doi.org/10.3767/persoonia.2018.40.01

Sandoval-Denis M, Lombard L, Crous PW (2019) Back to the roots: A reappraisal of *Neocosmospora*. Persoonia 43(1): 90–185. https://doi.org/10.3767/persoonia.2019.43.04

Silva S, Costa M, Cardoso A, Nascimento L, Barroso K, Nunes G, Pfenning L, Ambrósio M (2023) *Fusarium falciforme* and *Fusarium suttonianum* cause root rot of melon in Brazil. Plant Pathology 72(4): 721–730. https://doi.org/10.1111/ppa.13701

Snyder WC, Hansen HN (1940) The species concept in *Fusarium*. American Journal of Botany 27(2): 64–67. https://doi.org/10.1002/j.1537-2197.1940.tb14217.x

Summerell BA (2019) Resolving *Fusarium*: Current status of the genus. Annual Review of Phytopathology 57(1): 323–339. https://doi.org/10.1146/annurev-phyto-082718-100204

Taylor JW, Jacobson DJ, Kroken S, Kasuga T, Geiser DM, Hibbett DS, Fisher MC (2000) Phylogenetic species recognition and species concepts in fungi. Fungal Genetics and Biology 31(1): 21–32. https://doi.org/10.1006/fgbi.2000.1228

Thompson RS, Aveling TAS, Blanco Prieto R (2013) A new semi-selective medium for *Fusarium graminearum*, *F. proliferatum*, *F. subglutinans* and *F. verticillioides* in maize seed. South African Journal of Botany 84: 94–101. https://doi.org/10.1006/fgbi.2000.1228

Tian LY, Lian T, Ke SK, Qin CS, Xu JJ, Zhao DY, Qiu HL, Yang H, Jin XF, Li NL (2019) Fungal diseases of Chinese fir in northern Guangdong. 粤北地区杉木真菌性病害种类. Forestry and Environmental Sciences 35(04): 90–96.

Torres-Cruz TJ, Whitaker BK, Proctor RH, Broders K, Laraba I, Kim H-S, Brown DW, O'Donnell K, Estrada-Rodríguez TL, Lee Y-H, Cheong K, Wallace EC, McGee CT, Kang S, Geiser DM (2022) FUSARIUM-ID v.3.0: An updated, downloadable resource for *Fusarium* species identification. Plant Disease 106(6): 1610–1616. https://doi.org/10.1094/PDIS-09-21-2105-SR

Toussoun TA, Nelson PE (1968) *Fusarium*: A Pictorial Guide to the Identification of *Fusarium* Especies According to the Taxonomic System of Snyder and Hansen. The Pa Sta. Univ. Press., University Park, London, 51 pp.

Vismer HF, Marasas WF, Rheeder JP, Joubert JJ (2002) *Fusarium dimerum* as a cause of human eye infections. Medical Mycology 40(4): 399–406. https://doi.org/10.1080/mmy.40.4.399.406

Wang J, Cen B, Jiang Z, Peng S, Tong Z, Li G (1995) Identification of the pathogen which causes Chinese fir shoot blight. 杉木枯梢病的病原鉴定. Journal of South China Agricultural University 16(4): 47–49.

Wang M, Crous PW, Sandoval-Denis M, Han S-L, Liu F, Liang J, Duan W, Cai L (2022) *Fusarium* and allied genera from China: Species diversity and distribution. Persoonia 48(1): 1–53. https://doi.org/10.3767/persoonia.2022.48.01

Wollenweber HW, Reinking OA (1935) Die Fusarien: Ihre Beschreibung, Schadwirkung und Bekämpfung.

Wu SF, Zeng B, Zheng C, Mu XC, Zhang Y, Hu J, Zhang S, Gao CF, Shen JL (2018) The evolution of insecticide resistance in the brown planthopper (*Nilaparvata lugens*

Stål) of China in the period 2012–2016. Scientific Reports 8(1): e4586. https://doi.org/10.1038/s41598-018-22906-5

Xu YM, Liu YJ (2017) First report of *Nigrospora sphaerica* causing leaf blight on *Cunninghamia lanceolata* in China. Plant Disease 101(2): e389. https://doi.org/10.1094/PDIS-09-16-1229-PDN

Zeng ZQ, Zhuang WY (2023) Three new species of *Fusicolla* (Hypocreales) from China. Journal of Fungi 9(5): e572. https://doi.org/10.3390/jof9050572

Zhang D, Gao FL, Jakovli I, Zou H, Wang GT (2020) PhyloSuite: An integrated and scalable desktop platform for streamlined molecular sequence data management and evolutionary phylogenetics studies. Molecular Ecology Resources 20(1): 348–355. https://doi.org/10.1111/1755-0998.13096

Zhao L, Wei X, Huang CX, Yi JP, Deng JX, Cui MJ (2022) *Fusarium citri-sinensis* sp. nov. (Ascomycota: Nectriaceae) isolated from fruit of *Citrus sinensis* in China. Phytotaxa 555(3): 259–266. https://doi.org/10.11646/phytotaxa.555.3.5

Zheng W, Chen J, Hao Z, Shi J (2016) Comparative analysis of the chloroplast genomic information of *Cunninghamia lanceolata* (Lamb.) Hook with sibling species from the genera *Cryptomeria* D. Don, *Taiwania* Hayata, and *Calocedrus* Kurz. International Journal of Molecular Sciences 17(7): e1084. https://doi.org/10.3390/ijms17071084

Zhou H, Hou CL (2019) Three new species of *Diaporthe* from China based on morphological characters and DNA sequence data analyses. Phytotaxa 422(2): 157–174. https://doi.org/10.11646/phytotaxa.422.2.3

Supplementary material 1

Supplementary data

Authors: Jiao He, De-Wei Li, Wen-Li Cui, Li-Hua Zhu, Lin Huang

Data type: docx

Explanation note: **table S1.** Fungal cultures isolated from Chinese fir in this study. **table S2.** Genes/region and respective primer pairs used in the study. **table S3.** Nucleotide substitution models used in the phylogenetic analyses. **fig. S1.** *Fusarium concentricum* (SJ1-10). A–D, Colonies on PDA, SNA, OMA, and CMA, respectively, after 5 days at 24°C in the dark; E–F, sporodochia formed on PDA and the surface of carnation leaves, respectively; G–H, aerial conidiophores; I–J, sporodochial conidiophores, phialides, and conidia; K–L, aerial phialides and conidia; M, microconidia (0–1-septate) and macroconidia (3–5-septate). **fig. S2.** *Fusarium fujikuroi* (HN43-17-1). A–D, Colonies on PDA, SNA, OMA, and CMA, respectively, after 5 days at 24°C in the dark; E–H, aerial conidiophores, phialides, and microconidia; H, microconidia (0-septate); I, chlamydospore.

Link: https://doi.org/10.3897/mycokeys.101.113128.suppl1